NATIONAL ADVISORY COMMITTEE
FOR AERONAUTICS

TECHNICAL NOTE 4262

ANALYSIS OF TURBULENT FLOW AND HEAT TRANSFER ON A

FLAT PLATE AT HIGH MACH NUMBERS WITH

VARIABLE FLUID PROPERTIES

By R. G. Deissler and A. L. Loeffler, Jr.

Lewis Flight Propulsion Laboratory
Cleveland, Ohio

Washington
April 1958

NATIONAL ADVISORY COMMITTEE FOR AERONAUTICS

TECHNICAL NOTE 4262

ANALYSIS OF TURBULENT FLOW AND HEAT TRANSFER ON A FLAT PLATE

AT HIGH MACH NUMBERS WITH VARIABLE FLUID PROPERTIES

By R. G. Deissler and A. L. Loeffler, Jr.

SUMMARY

A previous analysis of turbulent heat transfer and flow with variable fluid properties in smooth passages is extended to flow over a flat plate at high Mach numbers. Velocity and temperature distributions are calculated for a boundary layer in which the effects of both frictional heating and external heat transfer are appreciable. The viscosity and thermal conductivity are assumed to vary as a power of the temperature, while the Prandtl number and specific heat are taken as constant. Skin-friction and heat-transfer coefficients are calculated and compared with the incompressible values. The relation between boundary-layer thickness and distance along the plate is obtained for various Mach numbers. The analytical results are compared with representative experimental data.

INTRODUCTION

The current emphasis on high-speed flight has caused much interest in research on compressible boundary layers. The skin friction in high Mach number flight constitutes a large part of the total drag. There-fore, the accurate prediction of skin friction is desirable for the design of high-speed aircraft. Prediction of heat-transfer coefficients in high Mach number flow is also important, because frictional heating of the surface necessitates cooling to prevent structural failures.

The prediction of laminar boundary layers from the basic equations of momentum, energy, and continuity has reached a high state of development. A considerable amount of analytical work on turbulent boundary layers has also been carried out. In the turbulent case, however, the results of the various analyses disagree markedly because of the different assumptions made by the various authors. These analyses are reviewed in references 1 to 3. The introduction of assumptions into the treatment of turbulent boundary layers is at present unavoidable, since solving the problem from the instantaneous equations of momentum, energy, and continuity alone is not yet possible. In some respects, however, the model

used for solving the problem might be improved. In nearly all the analyses, the flow is divided into a laminar region, where turbulence is supposed to be absent, and a fully turbulent region. The effect of variation of fluid properties on the laminar region is generally neglected. Measurements of turbulent velocity profiles indicate that considerable turbulent shear exists within the so-called laminar layer (ref. 4), so that a more realistic model for the region close to the wall than that used in previous analyses is desirable.

A somewhat improved treatment of the region close to the wall is given in references 4 to 6, where the effects of turbulence and of variable fluid properties in this region are considered. In the region away from the wall the von Kármán similarity expression has been considered the most reasonable expression available (ref. 7). In reference 8, fully developed turbulent flow and heat transfer in smooth passages for air with variable properties are analyzed, and the results agree well with experimental data. The analysis is extended to the entrance regions of passages and to high Prandtl numbers in references 9 and 10, where good agreement with experiment is again obtained. Since the analyses apply well to entrance regions, the assumptions made in the analyses should apply also to a compressible boundary layer. The analysis is extended to flow and heat transfer in a boundary layer at high Mach numbers in this paper. (Some preliminary results were presented in ref. 11.) The variation of properties due both to frictional heating and to external heat transfer is considered. The viscosity and thermal conductivity are assumed to vary as a power of the temperature, while the Prandtl number and specific heat are taken as constant.

SYMBOLS

A   constant

a   ratio of diffusivities, ϵ_h/ϵ

B   constant

C   constant

C_f friction coefficient, $2\tau_w/\rho_\delta u_\delta^2$

c_p specific heat of fluid at constant pressure

D   constant

d   exponent for viscosity variation with temperature, taken as 0.68 for air

E   constant

H   enthalpy

h   heat-transfer coefficient, $q_w/(t_w - t_{aw})$

k   thermal conductivity

M_δ Mach number based on free-stream properties and velocity, $u_\delta/\sqrt{\gamma R t_\delta}$

n   constant, 0.109

Pr   Prandtl number, $c_p\mu/k$

q   heat transfer in y-direction per unit time per unit area

R   perfect gas constant

Re_x Reynolds number based on x, $xu_\delta\rho_\delta/\mu_\delta$

Re_θ Reynolds number based on θ, $\theta u_\delta\rho_\delta/\mu_\delta$

St   Stanton number, $h/c_p u_\delta\rho_\delta$

T   total temperature, $t + (u^2/2c_p)$, deg abs

T^+ total-temperature parameter, $\dfrac{(t_w - T)c_p\tau_w}{q_w\sqrt{\tau_w/\rho_w}} = \dfrac{1 - (T/t_w)}{\beta}$

t   static temperature, deg abs

t^+ temperature parameter, $\dfrac{(t_w - t)c_p\tau_w}{q_w\sqrt{\tau_w/\rho_w}} = \dfrac{1 - (t/t_w)}{\beta}$

$t^{+\prime}$ temperature parameter, $\dfrac{2(t_w - t)c_p\rho_w}{\tau_w} = \dfrac{1 - (t/t_w)}{\alpha}$

u   velocity in x-direction

u^+ velocity parameter, $u/\sqrt{\tau_w/\rho_w}$

v   velocity in y-direction

x   longitudinal distance along plate

y distance perpendicular from plate

y^+ wall distance parameter, $\dfrac{y\sqrt{\tau_w/\rho_w}}{\mu_w/\rho_w}$

y_1^+ lowest value of y^+ for which equation for region away from wall applies

α frictional-heating parameter, $\tau_w/2c_p t_w \rho_w$

β heat-transfer parameter, $\dfrac{q_w\sqrt{\tau_w/\rho_w}}{c_p t_w \tau_w}$

γ ratio of specific heats, taken as 1.400 for air

δ flow boundary-layer thickness

δ^+ flow boundary-layer-thickness parameter, $\dfrac{\delta\sqrt{\tau_w/\rho_w}}{\mu_w/\rho_w}$

δ_h thermal boundary-layer thickness

δ_h^+ thermal boundary-layer-thickness parameter, $\dfrac{\delta_h\sqrt{\tau_w/\rho_w}}{\mu_w/\rho_w}$

ϵ eddy diffusivity of momentum

ϵ_h eddy diffusivity of heat

η temperature-recovery factor, $\dfrac{t_{aw} - t_\delta}{u_\delta^2/2c_p}$

θ momentum thickness, $\displaystyle\int_0^\delta \frac{\rho}{\rho_\delta}\frac{u}{u_\delta}\left(1 - \frac{u}{u_\delta}\right)dy$

θ^+ momentum-thickness parameter, $\dfrac{\theta\sqrt{\tau_w/\rho_w}}{\mu_w/\rho_w}$

$\varkappa$ constant, 0.36

μ viscosity

ρ density

τ shear stress, force per unit area

Subscripts:

aw   pertaining to adiabatic wall conditions

i   incompressible; constant fluid properties

w   pertaining to wall

δ   pertaining to edge of boundary layer or free stream

l   pertaining to edge of wall layer

Superscripts:

*   reference

'   pertaining to fluctuations from time average except in $t^{+'}$

―   time-averaged value

ANALYSIS AND DISCUSSION

Basic Equations

The instantaneous velocities, temperature, and fluid properties in the equations of momentum, energy, and continuity can be divided into mean and fluctuating components. If time averages are taken, the following equations for shear stress and heat transfer, applicable to flow in a boundary layer, are obtained (appendix A):

$$\tau = \mu \frac{du}{dy} - \rho \,\overline{u'v'} \tag{1}$$

$$q = -k \frac{dt}{dy} + \rho c_p \,\overline{t'v'} - u\mu \frac{du}{dy} + u\rho \,\overline{u'v'} \tag{2}$$

where constant specific heat is assumed. The bars denote time averages, and the primes indicate fluctuating components. Equations (1) and (2) are the same as equations (A9) and (A14) in appendix A if the bars over the time-averaged velocities, temperatures, and properties are dropped. The various terms in equations (1) and (2) may be interpreted as follows:

$\mu \dfrac{du}{dy}$ molecular shear stress

$-\rho \,\overline{u'v'}$ turbulent shear stress

$-k \dfrac{dt}{dy}$ molecular heat transfer

$\rho c_p \overline{t'v'}$ turbulent heat transfer

$-u\mu \dfrac{du}{dy}$ molecular dissipation

$u\rho \overline{u'v'}$ turbulent dissipation

Equations (1) and (2) suggest the form of the turbulent transfer equations but contain the unknown quantities $\overline{u'v'}$ and $\overline{t'v'}$, so that assumptions must be made before solutions can be obtained. For making these assumptions it is convenient to introduce the relations

$$\overline{u'v'} \equiv -\epsilon \frac{du}{dy} \quad \text{and} \quad \overline{t'v'} \equiv -\epsilon_h \frac{dt}{dy}$$

where ϵ and ϵ_h are the eddy diffusivities for momentum and heat transfer, the values of which depend upon the amount and kind of turbulent mixing at a point. When these relations are introduced, equations (1) and (2) become

$$\tau = (\mu + \rho\epsilon) \frac{du}{dy} \tag{3}$$

$$q = -(k + \rho c_p \epsilon_h) \frac{dt}{dy} - u(\mu + \rho\epsilon)\frac{du}{dy} \tag{4}$$

The physical significance of ϵ and ϵ_h lies in the fact that $\epsilon/(\mu/\rho)$ is the ratio of turbulent to molecular shear stress (ref. 12), and $\epsilon_h/(k/\rho c_p)$ is the ratio of turbulent to molecular heat transfer. Equations (3) and (4) can be written in dimensionless form as

$$\frac{\tau}{\tau_w} = \left(\frac{\mu}{\mu_w} + \frac{\rho}{\rho_w} \frac{\epsilon}{\mu_w/\rho_w} \right) \frac{du^+}{dy^+} \tag{5}$$

and

$$\frac{q}{q_w} = \left(\frac{k}{k_w} \frac{1}{Pr_w} + \frac{\rho}{\rho_w} a \frac{\epsilon}{\mu_w/\rho_w} \right) \frac{dt^+}{dy^+} - 2 \frac{\alpha}{\beta} u^+ \left(\frac{\mu}{\mu_w} + \frac{\rho}{\rho_w} \frac{\epsilon}{\mu_w/\rho_w} \right) \frac{du^+}{dy^+} \tag{6}$$

The subscripts w refer to values at $y = 0$; that is, at the wall. The quantity α is a frictional-heating parameter that is an indication of the variation of properties due to frictional heating, and β is a heat-flux parameter that is an indication of the variation of properties due to heat transfer. The parameter α is always positive or zero, a value of zero characterizing low-speed flow (i.e., $M_\delta = 0$). A zero value of β refers to a vanishingly small heat transfer or an insulated plate.

A positive value of β indicates heating of the fluid, while negative β means that the fluid is being cooled. It is sometimes convenient to write equation (6) in the following alternative dimensionless form:

$$\frac{\beta}{\alpha}\frac{q}{q_w} = \left(\frac{k}{k_w}\frac{1}{Pr_w} + \frac{\rho}{\rho_w}a\frac{\epsilon}{\mu_w/\rho_w}\right)\frac{dt^{+\prime}}{dy^+} - 2u^+\left(\frac{\mu}{\mu_w} + \frac{\rho}{\rho_w}\frac{\epsilon}{\mu_w/\rho_w}\right)\frac{du^+}{dy^+} \quad (7)$$

This equation is particularly convenient when $\beta = 0$, for which case equation (6) becomes indeterminate.

Expressions for Eddy Diffusivity

In order to make practical use of equations (5) to (7), the eddy diffusivity ϵ must be evaluated for each portion of the flow. For this purpose the boundary layer is divided into two portions termed the "region away from the wall" and the "region close to the wall."

Region away from wall. - In the region away from the wall, it is assumed that the turbulence at a point is a function mainly of local conditions - that is, of the relative velocities in the vicinity of the point (ref. 13). This is probably not a good assumption in the region near the edge of the boundary layer, where considerable diffusion of the turbulence occurs (ref. 14) and, in addition, the turbulence is intermittent. However, in that outer region the velocity or temperature gradients are so small with respect to these gradients nearer the wall that the error in calculated velocities or temperatures should not be large. A Taylor series expansion for u as a function of transverse distance, then, indicates that ϵ is a function of du/dy, d^2u/dy^2, d^3u/dy^3, and so forth. If, as a first approximation, ϵ is considered as a function only of the first and second derivatives, and dimensional analysis is applied,

$$\epsilon = \epsilon\left(\frac{du}{dy}, \frac{d^2u}{dy^2}\right) = \chi^2\frac{\left(\frac{du}{dy}\right)^3}{\left(\frac{d^2u}{dy^2}\right)^2} \quad (8)$$

This expression was obtained by von Kármán and is generally known as the Kármán similarity hypothesis (ref. 7). The constant χ is to be determined experimentally.

Region close to wall. - In the region close to the wall it is assumed that ϵ is a function only of quantities measured relative to the

wall - that is, of u and y.[1] This assumption includes, to a first
approximation, an effect of the derivative du/dy. Since the flow be-
comes very nearly laminar as the wall is approached, the first deriva-
tive approaches the value u/y and hence may be omitted, since u and
y already appear in the functional relation. By using dimensional
analysis,

$$\epsilon = \epsilon(u,y) = n^2 uy \tag{9}$$

where n is an experimental constant.

Equations (8) and (9) can be considered as reasonable first approx-
imations for ϵ. Whether these approximations are adequate or not can
at present be determined only by experiment.

Determination of experimental constants. - The constants n and $\varkappa$
were determined from pipe data in which the properties were essentially
constant. Equation (5), with equation (8) or (9), was integrated (con-
stant properties and τ) for the regions close to and away from the wall
in reference 4. The molecular shear stress was neglected in the region
away from the wall, and the well-known Kármán-Prandtl logarithmic equa-
tion was obtained in that region. In matching the two solutions it was
assumed that the velocity is continuous at the junction of the two
regions.

The integrated equations (ref. 4) for the regions close to and away
from the wall are plotted in figure 1 with the constants n = 0.109 and
$\varkappa = 0.36$ determined from pipe data (refs. 4 and 14). The data indicate
that the equation for the region close to the wall applies for $y^+ < 26$,
and the equation for the region away from the wall applies for $y^+ > 26$.
Included in the plot are data for a low-speed boundary layer with zero
pressure gradient from reference 15. The agreement with the curve is
satisfactory.

The values for the constants n = 0.109 and $\varkappa = 0.36$ should apply
to flow with variable as well as constant properties if the basic assump-
tions made for ϵ in the preceding sections apply to variable properties;
that is, if $\epsilon = \epsilon(u,y)$ close to the wall and $\epsilon = \epsilon(du/dy, d^2u/dy^2)$
away from the wall. The constant y_1^+, however, requires further consid-
eration and is discussed in the next section.

----

[1] Reference 10 shows that the kinematic viscosity has an effect on
ϵ in the region very close to the wall. However, that effect becomes
important only for heat or mass transfer at Prandtl or Schmidt numbers
appreciably greater than 1.

Additional Assumptions

In addition to the assumptions for eddy diffusivity discussed in the preceding section, several additional assumptions must be made for solving equations (5) to (7).

Variation of properties with temperature. - For gases, the viscosity varies approximately as t^d, where d has an average value of 0.68 for temperatures between 0° and 2000° F. The Prandtl number (Pr = 0.73) and specific heat c_p are assumed constant, because their variations with temperature are of a lower order of magnitude than the variations of the other properties. If c_p and Prandtl number are considered constant, the thermal conductivity k will vary with temperature in the same way as the viscosity, or as t^d. For constant pressure across the boundary layer, the density ρ is inversely proportional to t.

With the preceding assumptions, the property ratios in equations (5) to (7) can be written as

$$\frac{\mu}{\mu_w} = \frac{k}{k_w} = \left(\frac{t}{t_w}\right)^d = \left(\frac{t}{t_w}\right)^{0.68} \tag{10}$$

$$\frac{\rho}{\rho_w} = \frac{1}{t/t_w} \tag{11}$$

From the definitions of β and t^+,

$$\frac{t}{t_w} = 1 - \beta t^+ \tag{12}$$

or, if equation (7) rather than equation (6) is used,

$$\frac{t}{t_w} = 1 - \alpha t^{+'} \tag{13}$$

The property ratios in equations (5) to (7) can therefore be written in terms of β and t^+ or α and $t^{+'}$.

Variations of τ and q across boundary layer. - The momentum equation (A7) indicates that, for a flat plate (zero pressure gradient), $d\tau/dy = d(\mu du/dy)/dy = 0$ at the wall. Since τ is zero at the edge of the boundary layer, the actual variation of τ across the boundary layer might be expected, in general, to lie between a linear variation $(\tau/\tau_w = 1 - (y/\delta))$ and $\tau/\tau_w = 1$. Data on low-speed isothermal

flow over a flat plate (ref. 15) show that this type of variation does exist, except in a narrow region near the edge of the boundary layer. For determining the sensitivity of the velocity or temperature profile to shear-stress variation, it should therefore be sufficient to compare the profiles for a constant and for a linearly varying shear stress. Appendix B shows that $\tau/\tau_w = q/q_w$ for a flat plate if the Prandtl number is 1.

Figure 2 shows u^+ or T^+ plotted against y^+ for a Prandtl number of 1 for both a constant and a linearly varying shear stress and heat transfer, where T^+ is the total-temperature parameter. Curves are shown for $\beta = 0$ and $\alpha = 0$, 0.003, and 0.008, which cover much of the range of Mach number and Reynolds number of interest. The equations for calculating the curves are given in appendix D. The equation for the region away from the wall was taken to apply for $y^+ > 30$ rather than > 26 when the shear stress was variable, in order to give better agreement with the data for constant properties. The curve for $\alpha = 0.008$ is cut off at the point shown because the Mach number becomes infinite, as can be seen from equation (D3) (for $au^{+2} = 1$). The curves indicate that variable shear stress and heat transfer have but a slight effect on the velocity and temperature profiles. Similar curves were obtained in figure 11 of reference 6 for $\beta \neq 0$ and $\alpha = 0$. The same conclusions should apply to Prandtl numbers differing slightly from 1, so that the effects of the variations of τ and q across the boundary layer are neglected for solving equations (5) to (7).

Ranges of applicability of equations for flow close to and away from wall. - It was determined from the data for constant properties that the lowest value of y^+ for which the equation for the region away from the wall applies is $y_1^+ = 26$ when the variation of shear stress with y is neglected and the molecular shear stress is neglected in the region away from the wall. The question arises as to how y_1^+ varies when the properties are variable. The simplest assumption is that y_1^+ is constant and equal to 26. This assumption, which implies that the wall properties govern the thickness of the wall layer $\left(y_1^+ \equiv y_1\sqrt{\tau_w/\rho_w}/(\mu_w/\rho_w)\right)$, is similar to von Kármán's assumption (ref. 16). Figure 12 of reference 6 shows that essentially the same curves are obtained when the molecular shear stress is neglected in the region away from the wall as when it is considered, the difference being that, when the molecular shear stress is included, y_1^+ has the constant value of 16 rather than 26.

Another assumption, which might be somewhat more reasonable than assuming y_1^+ constant, is that y_1^+ occurs at a given constant ratio of turbulent to molecular shear stress $\epsilon/(\mu/\rho)$. That is, the turbulence changes from that described by equation (9) to that described by

equation (8) when the ratio of turbulent to molecular shear stress reaches a certain value. In this case the more complete equations are used for the region away from the wall, in which the molecular shear-stress and heat-transfer terms are retained and the slopes of the equations for flow close to and away from the wall are matched at y_1^+ ($y_1^+ = 16$ for $\beta = \alpha = 0$).

In figure 3, u^+ or T^+ is plotted against y^+ for a Prandtl number of 1 using the two assumptions for y_1^+ discussed in the preceding paragraphs. Curves are shown for $\beta = 0$ and $\alpha = 0$, 0.003, and 0.008. The equations for calculating the curves are given in appendix C. The curves indicate that the velocity and temperature profiles are apparently insensitive to the assumption used for y_1^+. Similar results were obtained in figure 13 of reference 6 for $\beta \neq 0$ and $\alpha = 0$. The simpler procedure of neglecting the molecular shear stress and heat transfer in the region away from the wall and assuming $y_1^+ = $ constant $= 26$ is therefore adopted in the following calculations.

Ratio of eddy diffusivities for heat and momentum transfer. - In most analyses the ratio of eddy diffusivities a that occurs in equations (6) and (7) is set equal to 1; that assumption has given heat-transfer coefficients in good agreement with experiment (ref. 8). It is of interest that Prandtl's mixing-length theory, which assumes that a turbulent particle moves a given distance and then suddenly mixes with the fluid and transfers its heat and momentum, gives a value of a = 1. Although the actual turbulence mechanism may be more complicated than indicated by that theory, it does indicate that a value of a on the order of 1 is not unreasonable.

In the present analysis the assumption of a = 1 is retained, but in some cases the calculations are also carried out for a = 1.07 in order to determine the effect of varying a. A ratio of diffusivities of 1.07 was obtained from some preliminary experiments on recovery factors for fully developed flow in a tube.

Velocity and Temperature Distributions in Boundary Layers

For obtaining velocity and temperature distributions close to the wall, equations (9) to (13) are substituted into equations (5) to (7). Equations (5) and (6) become, in integral form, with $\tau/\tau_w = q/q_w = 1$,

$$u^+ = \int_0^{y^+} \frac{dy^+}{(1 - \beta t^+)^d + \dfrac{1}{1 - \beta t^+} n^2 u^+ y^+} \tag{14}$$

$$t^+ = \int_0^{y^+} \frac{\left(1 + 2\frac{\alpha}{\beta}u^+\right)dy^+}{\frac{(1-\beta t^+)^d}{Pr} + \frac{a}{1-\beta t^+}n^2 u^+ y^+} \tag{15}$$

Equations (14) and (15) can be solved simultaneously by iteration; that is, assumed relations between u^+ and y^+ and t^+ and y^+ are substituted into the right sides of the equations, and new values of u^+ and t^+ are calculated by numerical integration. These new values are then substituted into the right sides of the equations and the process is repeated until the values of u^+ and t^+ do not change appreciably. Equations (14) and (15) give the relations among u^+, t^+, and y^+ for various values of α and β for flow close to the wall $(y^+ < 26)$. For $\beta = 0$ and $\alpha \neq 0$, t^+ becomes infinite, so that equations (5) and (7) must be used. These equations, with equation (13), become

$$u^+ = \int_0^{y^+} \frac{dy^+}{(1-\alpha t^{+\prime})^d + \frac{1}{1-\alpha t^{+\prime}}n^2 u^+ y^+} \tag{16}$$

$$t^{+\prime} = \int_0^{y^+} \frac{\left(\frac{\beta}{\alpha} + 2u^+\right)dy^+}{\frac{(1-\alpha t^{+\prime})^d}{Pr} + \frac{1}{1-\alpha t^{+\prime}}n^2 u^+ y^+} \tag{17}$$

Equations (16) and (17) are solved similarly to equations (14) and (15).

In the region away from the wall, the molecular shear stress and molecular heat transfer are neglected. Dividing equation (6) by equation (5) gives, with $\tau/\tau_w = q/q_w = 1$,

$$1 + 2\frac{\alpha}{\beta}u^+ = a\frac{dt^+}{du^+} \tag{18}$$

Integrating equation (18) from y_1^+ to y^+ gives

$$t^+ = t_1^+ + \frac{u^+}{a} - \frac{u_1^+}{a} + \frac{\alpha}{\beta a}u^{+2} - \frac{\alpha}{\beta a}u_1^{+2} \tag{19}$$

From equations (11), (12), and (19),

$$\frac{\rho}{\rho_w} = \frac{1}{1 - \beta t_1^+ + \dfrac{\beta u_1^+}{a} + \dfrac{\alpha}{a} u_1^{+2} - \dfrac{\beta u^+}{a} - \dfrac{\alpha}{a} u^{+2}}$$ (20)

Substitution of equations (8) and (20) into (5) and one integration give, for the region away from the wall,

$$K_a \frac{du^+}{dy^+} = e^{-\dfrac{\varkappa}{\sqrt{\alpha/a}} \sin^{-1}\left[\dfrac{2\alpha u^+ + \beta}{\sqrt{\beta^2 + 4\alpha(a - a\beta t_1^+ + \beta u_1^+ + \alpha u_1^{+2})}}\right]}$$ (21)

By letting

$$z = \frac{\varkappa}{\sqrt{\alpha/a}} \sin^{-1}\left[\frac{2\alpha u^+ + \beta}{\sqrt{\beta^2 + 4\alpha(a - a\beta t_1^+ + \beta u_1^+ + \alpha u_1^{+2})}}\right]$$ (22)

and integrating equation (21),

$$y^+ = \frac{K_b e^z}{1 + \dfrac{\alpha}{a\varkappa^2}}\left(\cos \frac{\sqrt{\alpha/a}}{\varkappa} z + \frac{\sqrt{\alpha/a}}{\varkappa} \sin \frac{\sqrt{\alpha/a}}{\varkappa} z\right) + K$$ (23)

The constant K is evaluated in the usual way by letting $du^+/dy^+ = \infty$ at $y^+ = 0$ in equation (21) (ref. 7) and substituting (21) into (22) and (23) at $y^+ = 0$.[2] By using this procedure, $K = 0$. To determine K_b, set $u^+ = u_1^+$ when $y^+ = y_1^+$. Then,

$$y^+ = \frac{y_1^+ e^z \left[\cos\left(\dfrac{\sqrt{\alpha/a}}{\varkappa} z\right) + \dfrac{\sqrt{\alpha/a}}{\varkappa} \sin\left(\dfrac{\sqrt{\alpha/a}}{\varkappa} z\right)\right]}{e^{z_1}\left[\cos\left(\dfrac{\sqrt{\alpha/a}}{\varkappa} z_1\right) + \dfrac{\sqrt{\alpha/a}}{\varkappa} \sin\left(\dfrac{\sqrt{\alpha/a}}{\varkappa} z_1\right)\right]}$$ (24)

where z is given by equation (22) and z_1 is the value of z at $y_1^+ = 26$. Equations (22) and (24) give the relation between u^+ and y^+

---

[2]This assumption can be avoided by including the molecular shear stress and heat transfer in the region away from the wall and evaluating K by assuming a continuous velocity derivative at y_1^+ (fig. 12, ref. 6). This assumption gives essentially the same results as that made in the text.

for various values of α and β. The quantity t^+ can then be calculated from equation (19).

For $\beta = 0$ and $\alpha \neq 0$, t^+ becomes infinite, and $t^{+'} = (\beta/\alpha)t^+$ must be used. Equation (19) becomes, in terms of $t^{+'}$,

$$t^{+'} = t_1^{+'} - \frac{\beta}{\alpha a} u_1^+ - \frac{u_1^{+2}}{a} + \frac{\beta}{\alpha a} u^+ + \frac{u^{+2}}{a} \qquad (25)$$

Equations (22) and (24) apply to the case for $\beta = 0$ and $\alpha \neq 0$ if $\alpha t_1^{+'}$ is substituted for βt_1^+ in equation (22).

For $\alpha = 0$, equation (23) becomes indeterminate, and equation (21) for zero frictional heating from reference 6 can be used.

Typical velocity and temperature distributions for various values of the frictional-heating parameter α and of the heat-flux parameter β are presented in figures 4 to 6. Positive values of β correspond to heat addition to the air; negative values, to heat extraction. The curves of u^+ against y^+ (fig. 4) indicate considerable flattening of the velocity profile as either α or β increases positively. This is caused by the decreasing temperatures in the outer regions of the boundary layer compared with the wall temperature when either the Mach number is high (high α) or the heat transfer from the surface to the air is high. Thus, the density is higher in the outer regions of the boundary layer, with consequent flattening of the profile (eq. (5)). Negative values of β produce the opposite effect. For certain combinations of α and β (with β negative), the effect of β on the curves should tend to cancel the effect of α, and the resulting profile should not differ greatly from the $\alpha = \beta = 0$ curve. The curve for $\alpha = 0.002$, $\beta = -0.05$ in figure 4 is close to the curve for $\alpha = \beta = 0$. Included in figure 4 for comparison are experimental data from reference 17 for an α of 0.00176, $\beta = 0$, and a corresponding Mach number M_δ of 2.82. The data are in reasonable agreement with the predicted profiles.

In figure 5 T^+ is plotted against y^+ for various values of α and β. The total-temperature parameter T^+ is plotted rather than t^+, because the trends are somewhat more consistent, although some crossing over of the curves occurs even with T^+. For calculation purposes, a better representation can be obtained by plotting T^+ against u^+. The quantity T^+ is related to t^+ by the relation

$$T^+ = t^+ - \frac{\alpha}{\beta} u^{+2} \qquad (26)$$

Skin-Friction Coefficients

The skin-friction coefficient is defined as

$$C_f \equiv \frac{2\tau_w}{\rho_\delta u_\delta^2} \tag{27}$$

where the subscript δ refers to values outside the boundary layer. Equation (27) becomes, in dimensionless form,

$$C_f = \frac{\rho_w}{\rho_\delta}\frac{2}{u_\delta^{+2}} = \frac{2(1 - \alpha t_\delta^{+'})}{u_\delta^{+2}} = \frac{2(1 - \beta t_\delta^{+})}{u_\delta^{+2}} \tag{28}$$

For comparison with experimental data, it is convenient to introduce the momentum thickness,

$$\theta \equiv \int_0^\delta \frac{\rho}{\rho_\delta}\frac{u}{u_\delta}\left(1 - \frac{u}{u_\delta}\right)dy \tag{29}$$

which in dimensionless form is

$$\theta^+ = (1 - \alpha t_\delta^{+'})\int_0^{\delta^+} \frac{1}{1 - \alpha t^{+'}}\frac{u^+}{u_\delta^+}\left(1 - \frac{u^+}{u_\delta^+}\right)dy^+ \tag{30}$$

Then the Reynolds number based on the momentum thickness and free-stream properties is

$$Re_\theta \equiv \frac{\theta u_\delta \rho_\delta}{\mu_\delta} = \theta^+ u_\delta^+ \frac{\mu_w}{\mu_\delta}\frac{\rho_\delta}{\rho_w} \tag{31}$$

where the property ratios are obtained from equations (10) to (13). The Mach number for a perfect gas is

$$M_\delta = \frac{u_\delta}{\sqrt{\gamma R t_\delta}} = u_\delta^+ \sqrt{\frac{2\alpha}{(\gamma - 1)(t_\delta/t_w)}} \tag{32}$$

If values are given to α, β, and δ^+, where δ^+ is the value of y^+ at the edge of the flow boundary layer, then values of u_δ^+, t_δ^+, and so forth can be read from curves similar to those in figures 4 to 6. Values of C_f, Re_θ, and M_δ can then be calculated from equations (28), (31), and (32). This procedure assumes that the thermal and flow boundary

layers are of equal thickness. From the calculations in a later section, where relations between boundary-layer thickness and distance along the plate are calculated, it can be shown that this is a good assumption for gases when the thermal and flow boundary layers begin at the same point. For the case of $Pr = a = 1$ the assumption holds exactly, as can be seen by substituting $u^+ = T^+$ into equations (42) and (43), which are then identical.

Predicted skin-friction coefficients are plotted against Re_θ in figure 7 for various values of Mach number for an insulated plate ($\beta = 0$). These curves are for $\epsilon_h/\epsilon = a = 1$. The effect on the curves of changing a to 1.07 was negligible. The values of C_f decrease considerably as Mach number increases. Included in the plot are experimental data of a number of investigators for Mach numbers up to 4.93. In general, the data are in good agreement with the predicted curves.

The ratio of the friction coefficient to the incompressible coefficient is plotted against Mach number for various values of Re_θ for $\beta = 0$ in figure 8. The values of $C_f/C_{f,i}$ decrease with Re_θ, but at a decreasing rate. For comparison purposes the analytical curve of $C_f/C_{f,i}$ against M_δ for a value of Re_θ of 6000 is plotted in figure 9 together with data taken near this value of Re_θ.

If heat transfer occurs between the plate and the stream, it is convenient to specify the ratio of the actual wall temperature to the adiabatic wall temperature for a given Mach number and Re_θ. For an insulated plate the adiabatic wall temperature may be written as

$$t_{aw} = t_\delta + \eta \frac{u_\delta^2}{2c_p} \qquad (33a)$$

where η is the temperature-recovery factor, the calculation of which is discussed in the next section. Equation (33a) can be written in dimensionless form as

$$\frac{t_w}{t_{aw}} = \frac{1}{1 - \beta t_\delta^+ + \eta \alpha u_\delta^{+2}} \qquad (33b)$$

Figure 10 is similar to figure 7, except that the plate is now cooled ($t_w/t_{aw} = 0.5$). The trends are similar to those of figure 7, but all the curves are displaced upward. This increase in friction coefficient was also obtained for flow in a tube with cooling (ref. 5). Also included in this figure are wind-tunnel data (ref. 18) obtained at high Mach number using nitrogen as the working fluid. The agreement with theory appears to be within experimental error.

Figure 11 is similar to figure 8 but is for a value of 0.5 for t_w/t_{aw}. It is of interest to note from both figures 8 and 11 that the percentage effect of varying Reynolds number is much greater for the higher Mach numbers. Thus, figure 8 indicates that for a Mach number of 20 the value of $C_f/C_{f,i}$ for Re_θ of 10^5 is less than half that for Re_θ of 10^3.

Reference Temperatures and Extension of Results to

Greater Cooling Rates

The defining equation for reference temperature is

$$t^* = t_\delta + C(t_w - t_\delta) + D(t_{aw} - t_w) \qquad (34a)$$

where C and D are constants to be evaluated from theoretical or experimental results. Dividing equation (34a) by t_δ and assuming that the recovery factor is constant at 0.88 and that $\gamma = 1.40$ result in a more useful form of the equation:

$$\frac{t^*}{t_\delta} = (1 - C) + \left[(C - D)\frac{t_w}{t_{aw}} + D\right]\left(1 + 0.176\ M_\delta^2\right)$$

According to the concept of reference temperature, the relation between incompressible friction factor and Reynolds number should hold for variable-property flow if the properties are evaluated at the reference temperature. The results of this analysis could not be represented accurately in such a manner. It was necessary to write the incompressible relation in the form

$$C_{f,i} = \frac{E}{Re_\theta^{0.0744}}$$

where E is a constant. It should be noted that this is not the true incompressible relation and is used only for reference temperature purposes. If the properties are evaluated at the reference temperature, the result is

$$C_f = \frac{E}{Re_\theta^{0.0744}}\left(\frac{t^*}{t_\delta}\right)^{-0.875}$$

Dividing this equation by the previous one gives

$$\frac{c_f}{c_{f,i}} = \left(\frac{t^*}{t_\delta}\right)^{-0.875} \tag{34b}$$

For Re_θ of 10^5, evaluating the constants C and D in the reference temperature equation from the results in figures 8 and 11 and equation (34b) gives $C = 0.56$ and $D = 0.184$. The reference temperature can then be written

$$\frac{t^*}{t_\delta} = 0.44 + \left(0.376 \frac{t_w}{t_{aw}} + 0.184\right)\left(1 + 0.176 M_\delta^2\right) \tag{34c}$$

The results of the use of equations (34b) and (34c) are shown as dashed lines in figures 8 and 11. Thus, by use of equations (34b) and (34c) it should be possible to extend the results of this analysis to values of t_w/t_{aw} other than 1.0 and 0.5 if the value of Re_θ is near 10^5.

An estimate for lower Reynolds numbers may be obtained by first using the preceding method to find the friction factor at $Re_\theta = 10^5$ and then finding the ratios of friction factor at the desired Reynolds number to that at $Re_\theta = 10^5$ from figures 8 and 11. These ratios can then be interpolated or extrapolated to the desired value of t_w/t_{aw}. This procedure can be justified since the ratio does not vary greatly with t_w/t_{aw}.

Stanton Numbers and Recovery Factors

The Stanton number based on the difference between the wall and the adiabatic wall temperature, with properties evaluated at the free-stream temperature, is given by

$$St \equiv \frac{h}{c_p u_\delta \rho_\delta} = \frac{1}{t_\delta^+ u_\delta^+ \dfrac{\rho_\delta}{\rho_w}} \frac{1 - \dfrac{t_\delta}{t_w}}{1 - \dfrac{t_\delta}{t_w} - \eta \alpha u_\delta^{+2}} \tag{35}$$

where equation (33a) is used. The temperature and density ratios are determined from equations (11) and (12) or (13). For $\beta = 0$ and $\alpha \neq 0$, equation (35) becomes indeterminate. For that case set $1 - (t_\delta/t_w) = \alpha t_\delta^{+'}$ and $t_\delta^+ = (\alpha/\beta)t_\delta^{+'}$. With these substitutions equation (35) becomes

$$St = \frac{\beta}{\alpha u_\delta^+ (\rho_\delta/\rho_w)(t_\delta^{+'} - \eta u_\delta^{+2})} \tag{36}$$

From equations (7) and (5) $(q/q_w = \tau/\tau_w = 1)$,

$$t_\delta^{+'} = \frac{\beta}{\alpha} \int_0^{\delta^+} \frac{dy^+}{\dfrac{k}{k_w}\dfrac{1}{Pr_w} + \dfrac{\rho}{\rho_w} a \dfrac{\epsilon}{\mu_w/\rho_w}} + \int_0^{\delta^+} \frac{2u^+ \, dy^+}{\dfrac{k}{k_w}\dfrac{1}{Pr_w} + \dfrac{\rho}{\rho_w} a \dfrac{\epsilon}{\mu_w/\rho_w}} \tag{37}$$

The second integral in this equation can be replaced by $\left(t_\delta^{+'}\right)_{\beta=0}$. But equation (33a) can be written in dimensionless form as

$$\eta u_\delta^{+2} = \left(t_\delta^{+'}\right)_{\beta=0} \tag{38}$$

Substituting equations (37) and (38) into (36), with the second integral in equation (37) replaced by $\left(t_\delta^{+'}\right)_{\beta=0}$, gives

$$St = \frac{1}{u_\delta^+ \dfrac{\rho_\delta}{\rho_w} \displaystyle\int_0^{\delta^+} \frac{dy^+}{\dfrac{k}{k_w}\dfrac{1}{Pr_w} + \dfrac{\rho}{\rho_w} a \dfrac{\epsilon}{\mu_w/\rho_w}}} \tag{39}$$

For evaluating equation (39) in the region close to the wall, $\epsilon/(\mu_w/\rho_w) = n^2 u^+ y^+$. For the region away from the wall, ϵ could be obtained from equation (8). However, it is more convenient to obtain ϵ from equation (5), which for the region away from the wall becomes

$$\frac{\rho}{\rho_w}\frac{\epsilon}{\mu_w/\rho_w} = \frac{1}{du^+/dy^+}$$

Equation (39) can be used for $\beta = 0$ or $\beta \neq 0$. For given values of δ^+, α, and β, values of Stanton number, Mach number, t_w/t_{aw}, and Re_θ can be calculated from equations (39), (32), (33b), (30), (31), and (10) to (13).

Predicted Stanton numbers are plotted against Re_θ for various Mach numbers for $t_w/t_{aw} = 1$ in figure 12. The case of $t_w/t_{aw} = 1$ is a limiting case that can be approached as closely as desired by making the heat flux small. When $t_w/t_{aw} = 1$, there is no effect of variable

properties due to heat flux. The Stanton numbers in figure 12 show
trends similar to those of the friction coefficients in figure 7. In-
cluded in the figure are experimental data for low heat flux obtained by
a number of investigators. In general, the data are in good agreement
with the predicted curves. The curves in figure 12 are for $\epsilon_h/\epsilon = a = 1$.
Similar curves for an a of 1.07 were 3 to 5 percent higher for a Mach
number of 0, but the difference decreased at higher Mach numbers. The
curves for a = 1 are in slightly better agreement with the data than
those for a = 1.07.

The ratio of Stanton number to the incompressible Stanton number is
plotted against Mach number for various values of Re_θ for $t_w/t_{aw} = 1$
in figure 13. These curves are very nearly the same as those for
$C_f/C_{f,i}$ in figure 8.

Figure 14 is similar to figure 12, except that $t_w/t_{aw} = 0.5$. As
was the case for the friction coefficients in figure 10, the Stanton
numbers increase as t_w/t_{aw} decreases. The corresponding plot of
St/St_i against Mach number for various values of Re_θ and $t_w/t_{aw} = 0.5$
is shown in figure 15.

Temperature-recovery factors, as calculated from equation (38), are
shown in figure 16 for Mach numbers from 0 to 8. Curves are shown for
a = 1 and a = 1.07. The curves for a = 1.07 are in somewhat better
agreement with most of the experimental data than those for a = 1.
This does not mean that an a of 1.07 should be used for calculating
heat transfer or Stanton numbers. According to Reichardt's hypothesis,
the value of a should be close to 1 at the wall and increase with dis-
tance from the wall (ref. 12). The temperature profiles for calculating
heat-transfer coefficients are very steep near the wall, so that the im-
portant charges with distance take place near the wall where a is close
to 1. In the case of recovery factors, however, the plate is insulated,
so that the temperature gradient is zero at the wall. The gradients near
the wall will therefore be smaller than in the case of heat transfer, and
important changes of temperature with distance might occur in regions
away from the wall where a is somewhat greater than 1.

Figures 17(a) and (b) show the curves of the Reynolds analogy factor
$2St/C_f$ against Mach number for various Re_θ, for t_w/t_{aw} equal to 1.0
and 0.5, respectively. If Reynolds' analogy held strictly (Pr = a = 1),
the Stanton number would be equal to one-half the friction factor and
$2St/C_f$ would be unity. Figure 17 shows a variation of the Reynolds
analogy factor over the range 1.065 to 1.280. In general, $2St/C_f$ in-
creases with increasing Mach number and with decreasing Reynolds number
and increases slightly with decreasing t_w/t_{aw} at the higher Mach

numbers. These results are in approximate agreement with those of Rubesin (ref. 19), who estimated that $2St/C_f$ would be in the range 1.18 to 1.21 at least up to M_δ of 5.

To obtain approximate values of St as a function of Re_θ and M_δ for t_w/t_{aw} other than 1.0 and 0.5, it is recommended that the results of figure 17 be interpolated or extrapolated to give the value of $2St/C_f$ at the desired condition. Then C_f can be found from equations (34b) and (34c) as previously described, and thus the value of St is obtained.

Relation between Boundary-Layer Thickness and Distance along Plate

From the results given in the preceding sections, the skin friction or heat transfer for a given boundary-layer or momentum thickness can be calculated. In order to calculate the relations between thermal or flow boundary-layer thickness and distance along the plate, the well-known integral momentum and energy equations may be used. These equations may be written as follows for a flat plate (zero pressure gradient):

$$\tau_w = \frac{d}{dx} \int_0^\delta \left[\rho u (u_\delta - u) dy \right] \qquad (40)$$

$$q_w = \frac{d}{dx} \int_0^{\delta_h} \left[c_p \rho u (T - T_\delta) dy \right] \qquad (41)$$

If $\delta = \delta_h = 0$ for $x = 0$ and equations (40) and (41) are integrated with respect to x, they become, in dimensionless form,

$$Re_x = \int_0^{[\,]} \frac{\rho_\delta}{\rho_w} u_\delta^{+2} \, d \left[\frac{\mu_w}{\mu_\delta} \frac{1}{u_\delta^+} \int_0^{\delta^+} \frac{\rho}{\rho_w} u^+ (u_\delta^+ - u^+) dy^+ \right] \qquad (42)$$

$$Re_x = \int_0^{[\,]} T_\delta^+ u_\delta^+ \frac{\rho_\delta}{\rho_w} \, d \left[\left(\frac{\mu_w}{\mu_\delta} \right) \frac{1}{T_\delta^+} \int_0^{\delta_h^+} \frac{\rho}{\rho_w} u^+ (T_\delta^+ - T^+) dy^+ \right] \qquad (43)$$

where the bracket for the upper limit of integration refers to the value of the variable of integration at that point. These equations give the relations between δ^+ and Re_x and δ_h^+ and Re_x. The property ratios are obtained from equations (10) to (13).

Equation (42) can be written in the more convenient form

$$Re_x = 2 \int_0^{Re_\theta} \frac{dRe_\theta}{C_f} \qquad (44)$$

The Reynolds number based on momentum thickness Re_θ is plotted against Re_x, as found from equation (44), for an insulated plate in figure 18. The value of Re_θ decreases at a given Re_x as the Mach number increases if the free-stream properties remain constant. This is caused (eq. (44)) by the decrease of friction factor with increasing Mach number (fig. 7). Data included in figure 18 agree reasonably well with the analytical curves.

Figure 19 is similar to figure 18, except that $t_w/t_{aw} = 0.5$. For given values of Re_x and Mach number the values of Re_θ are generally a little higher for t_w/t_{aw} of 0.5 than for t_w/t_{aw} of 1. This trend can be understood from examination of equation (44), since C_f is higher for t_w/t_{aw} of 0.5 (fig. 10) than for t_w/t_{aw} of 1.0 (fig. 7).

Predicted skin-friction coefficients for an insulated plate are plotted against Re_x in figure 20. The trends with Mach number are similar to those obtained when C_f is plotted against Re_θ but are less pronounced, because the boundary-layer thickness at a given x decreases with increasing Mach number. Experimental data for low-speed flow included in the figure are in good agreement with the predicted curve for a Mach number of zero. Data for higher Mach numbers are also in reasonable agreement with the predicted curves but are somewhat more scattered than the data in figure 7, where C_f is plotted against Re_θ. This scatter is apparently caused by uncertainty as to the point at which the boundary layer actually starts in a supersonic flow.

In figure 21, the theoretical curves are replotted as $C_f/C_{f,i}$ against Mach number for various Reynolds numbers based on x. The effect on $C_f/C_{f,i}$ of varying Re_x becomes appreciable at high Mach numbers.

Stanton numbers for an insulated plate are plotted against Re_x for a Mach number of zero in figure 22. Curves for higher Mach numbers and for t_w/t_{aw} of 0.5 involve considerably more calculation and were not obtained.

Figures 23 and 24 are analogous to figures 20 and 21, respectively, except that they are for t_w/t_{aw} of 0.5. The friction factors, as expected, are higher for the larger rates of cooling.

Reference Temperature for Re_x Results

The customary use of a reference temperature concept requires that the Reynolds number dependence of C_f and of St be the same for all Mach numbers so that $C_f/C_{f,i}$ and St/St_i should not be functions of Reynolds number. Examination of the predicted curves of $C_f/C_{f,i}$ and St/St_i against Mach number as shown in figures 8, 11, 13, 15, 21, and 24 shows, however, that $C_f/C_{f,i}$ and St/St_i are strong functions of Reynolds number at the higher Mach numbers. Therefore, the present theory cannot be represented accurately by one reference temperature valid for all Reynolds numbers.

For purposes of comparison, however, the results obtained by using Eckert's suggested reference temperature (ref. 3) are shown in figures 21 and 24. Agreement with the present theory for $Re_x = 10^8$ is quite good. Use of Eckert's reference temperature method to solve for $C_f/C_{f,i}$, is recommended, then, if large values of Re_x (near 10^8) are considered. In order to solve for C_f, the value of $C_{f,i}$ can be taken from the curve for $M_\delta = 0$ in figure 20. An approximation (within 5 percent) to this case is

$$C_f = 0.0292 \ Re_x^{-0.151}$$

In order to solve for values of C_f at values of t_w/t_{aw} other than 1.0 and 0.5 and for values of Re_x other than 10^8, the same approximate procedure as recommended for Re_θ as the variable can be employed. For this case, however, instead of figures 8 and 11, figures 21 and 24 and Eckert's reference temperature should be utilized.

To obtain an approximate relation between Stanton number and Re_x the following procedure is recommended: Find the value of Re_θ corresponding to the specified Re_x by interpolation or extrapolation of figures 18 and 19. From this value of Re_θ find the Reynolds analogy factor by similar use of figure 17 for the specified values of t_w/t_{aw} and M_δ. This value of the Reynolds analogy factor and the value of C_f obtained as shown in the previous paragraph are sufficient to solve for the Stanton number for the specified conditions.

Closing Remarks

No attempt has been made in this analysis to include the effects of dissociation, shock waves, radiation, slip flow, or induced pressure gradients.

A rough estimate of the effect of dissociation may be inferred, as pointed out by Eckert (ref. 3), from the theory of laminar boundary layers. Thus, both Crown (ref. 20) and Moore (ref. 21) conclude that the effect of dissociation on friction factor and heat flux for the laminar boundary layer will be small if the wall temperature is less than the air dissociation temperature, which, even at a pressure of 0.0001 atmosphere, is above 3000° F. Their calculations were made for Mach numbers up to 20. Where dissociation is appreciable, it is recommended that the heat-transfer coefficients presented in this report be interpreted as based on an enthalpy difference instead of a temperature difference, Thus,

$$h = \frac{c_p q}{H_w - H_{aw}}$$

and

$$St = \frac{q}{(H_w - H_{aw})u_\delta \rho_\delta}$$

where H is the enthalpy.

Although in practice there would be a shock wave originating near the leading edge of the flat plate for high Mach numbers, the effect on temperature and pressure distributions appears too complicated to be taken into account. Therefore, constancy of free-stream pressure and temperature has been assumed.

The possibility of encountering slip flow at high Mach number must also be considered. According to Eckert (ref. 3) the assumption of a continuum is valid as long as the Knudsen number $\left[= \dfrac{\sqrt{\frac{\gamma \pi}{8}} M_\delta}{0.499 \, Re_\delta} \right]$ is less than 0.01. To obtain a conservative estimate for the range of conditions considered in this report, values of M_δ and Re_δ of 20 and 10^4, respectively, are used. For these values the Knudsen number is 0.00298, which is well below the criterion for slip flow.

SUMMARY OF RESULTS

The following results were obtained from the analysis of turbulent flow and heat transfer over a flat plate at high Mach numbers:

1. The frictional heating that occurs at high Mach numbers produced a flattening of the velocity profile, as does heating the plate by other means. Cooling the plate caused the velocity gradients near the outer edge of the boundary layer to increase.

2. The skin-friction coefficients and Stanton numbers at a given Reynolds number decreased as Mach number increased.

3. The curves for the ratio of friction coefficient to the incompressible coefficient against Mach number agreed closely with the curves for the ratio of Stanton number to incompressible Stanton number against Mach number.

4. Cooling the plate to offset the effects of frictional heating increased the friction coefficients and Stanton numbers.

5. Frictional heating at high Mach numbers produced a thinning of the boundary layer at a given position on the plate for the same free-stream properties.

6. The predicted friction coefficients and Stanton numbers agreed closely with representative experimental data.

7. The Reynolds number effect on both friction factor and Stanton number increases greatly with increasing Mach number.

Lewis Flight Propulsion Laboratory
National Advisory Committee for Aeronautics
        Cleveland, Ohio, January 17, 1958

APPENDIX A

DERIVATION OF TURBULENT MOMENTUM AND ENERGY EQUATIONS

Momentum Equation

The momentum equation for compressible boundary-layer flow past a flat plate can be written as

$$\rho u \frac{\partial u}{\partial x} + \rho v \frac{\partial u}{\partial y} = \frac{\partial}{\partial y}\left(\mu \frac{\partial u}{\partial y}\right) \tag{A1}$$

and the continuity equation as

$$\frac{\partial(\rho u)}{\partial x} + \frac{\partial(\rho v)}{\partial y} = 0 \tag{A2}$$

Time derivatives and pressure gradients are neglected in equations (A1) and (A2), as they drop out when time averages are taken.

The instantaneous quantities in equation (A1) are now replaced by their time averages and fluctuating components, which are written as

$$\left.\begin{aligned} u &= \overline{u} + u' & \rho &= \overline{\rho} + \rho' \\ v &= \overline{v} + v' & \mu &= \overline{\mu} + \mu' \end{aligned}\right\} \tag{A3}$$

and time averages are taken term by term. The following order-of-magnitude criteria are used for both the momentum and energy equations:

$$\frac{\partial}{\partial x} \approx O(1)$$

$$\frac{\partial}{\partial y} \approx O(\delta^{-1})$$

$$\overline{\rho},\ \overline{u},\ \overline{t} \approx O(1)$$

$$\overline{v} \approx O(\delta)$$

$$\overline{k},\ \overline{\mu} \approx O(\delta^2)$$

$$\overline{u'v'},\ \overline{\rho'v'},\ \text{etc.} \approx O(\delta)$$

$$\overline{\rho'u'v'},\ \overline{\rho'u'^2},\ \text{etc.} \approx O(\delta^{3/2})$$

$$\text{Double correlations containing } k' \text{ and } \mu' \approx O(\delta^3)$$

The first five of these criteria are the usual boundary-layer assumptions. The sixth results from assuming that the laminar and turbulent shear stresses are of the same order of magnitude. The seventh is consistent with the sixth, since a triple correlation should be roughly of the magnitude of a double correlation raised to the 3/2 power. The eighth appears justified since it might be expected that k' and μ' should be at least one-half order of magnitude less than $\bar{k}$ and $\bar{\mu}$.

With the preceding criteria, the time-averaged momentum equation becomes, on neglecting terms of magnitude δ and less,

$$\bar{\rho}\,\bar{u}\,\frac{\partial \bar{u}}{\partial x} + \left(\overline{\rho v} + \overline{\rho'v'}\right)\frac{\partial \bar{u}}{\partial y} = \frac{\partial}{\partial y}\left(\bar{\mu}\,\frac{\partial \bar{u}}{\partial y} - \bar{\rho}\,\overline{u'v'}\right) \tag{A4}$$

and the continuity equation,

$$\frac{\partial\left(\overline{\rho u}\right)}{\partial x} + \frac{\partial\left(\overline{\rho v}\right)}{\partial x} + \frac{\partial\left(\overline{\rho'v'}\right)}{\partial y} = 0 \tag{A5}$$

Considering the relation

$$\overline{\rho v} + \overline{\rho'v'} = \overline{\rho v} \tag{A6}$$

equations (A4) and (A5) can be rewritten

$$\overline{\rho u}\,\frac{\partial \bar{u}}{\partial x} + \overline{\rho v}\,\frac{\partial \bar{u}}{\partial y} = \frac{\partial}{\partial y}\left(\bar{\mu}\,\frac{\partial \bar{u}}{\partial y} - \bar{\rho}\,\overline{u'v'}\right) \tag{A7}$$

and

$$\frac{\partial\left(\overline{\rho u}\right)}{\partial x} + \frac{\partial\left(\overline{\rho v}\right)}{\partial y} = 0 \tag{A8}$$

Comparison of equations (A1) and (A7) leads to the definition of τ as

$$\tau = \bar{\mu}\,\frac{\partial \bar{u}}{\partial y} - \bar{\rho}\,\overline{u'v'} \tag{A9}$$

Energy Equation

The energy equation for compressible boundary-layer flow past a flat plate is

$$\rho u c_p\,\frac{\partial t}{\partial x} + \rho v c_p\,\frac{\partial t}{\partial y} = \frac{\partial}{\partial y}\left(k\,\frac{\partial t}{\partial y}\right) + \mu\left(\frac{\partial u}{\partial y}\right)^2 \tag{A10}$$

Time derivatives and pressure gradients are again neglected, as time-averaging cancels them. If the momentum equation (A1) is multiplied through by u and then added to equation (A10), the result is

$$\rho u \frac{\partial}{\partial x}\left(c_p t + \frac{u^2}{2}\right) + \rho v \frac{\partial}{\partial y}\left(c_p t + \frac{u^2}{2}\right) = \frac{\partial}{\partial y}\left(k \frac{\partial t}{\partial y} + \mu u \frac{\partial u}{\partial y}\right) \quad (A11)$$

where c_p is considered constant.

Again substituting for the instantaneous quantities the sum of the time-averaged and fluctuating components, and then neglecting terms of small order of magnitude on taking time averages, equation (A11) becomes

$$\bar{\rho}\bar{u} \frac{\partial}{\partial x}\left(c_p \bar{t} + \frac{\bar{u}^2}{2}\right) + \left(\bar{\rho}\bar{v} + \overline{\rho' v'}\right)\frac{\partial}{\partial y}\left(c_p \bar{t} + \frac{\bar{u}^2}{2}\right) =$$
$$\frac{\partial}{\partial y}\left(\bar{k}\frac{\partial \bar{t}}{\partial y} + \bar{\mu}\bar{u}\frac{\partial \bar{u}}{\partial y} - \bar{\rho}c_p \overline{v't'} - \bar{\rho}\bar{u}\,\overline{u'v'}\right) \quad (A12)$$

Again employing equation (A6), equation (A12) becomes

$$\bar{\rho}\bar{u} \frac{\partial}{\partial x}\left(c_p \bar{t} + \frac{\bar{u}^2}{2}\right) + \bar{\rho}\bar{v} \frac{\partial}{\partial y}\left(c_p \bar{t} + \frac{\bar{u}^2}{2}\right) =$$
$$\frac{\partial}{\partial y}\left(\bar{k}\frac{\partial \bar{t}}{\partial y} + \bar{\mu}\bar{u}\frac{\partial \bar{u}}{\partial y} - \bar{\rho}c_p \overline{v't'} - \bar{\rho}\bar{u}\,\overline{u'v'}\right) \quad (A13)$$

A comparison of equations (A11) and (A13) shows that

$$q = -\left(\bar{k}\frac{\partial \bar{t}}{\partial y} + \bar{\mu}\bar{u}\frac{\partial \bar{u}}{\partial y} - \bar{\rho}c_p \overline{v't'} - \bar{\rho}\bar{u}\,\overline{u'v'}\right) \quad (A14)$$

It should be noted that this treatment gives no density fluctuation terms in the expressions for τ and q. This same result was found by Van Driest (ref. 22) and by Rubesin (ref. 19). Combining $\overline{\rho'v'}$ with $\bar{\rho}\bar{v}$ and writing the sum as $\overline{\rho v}$ present no difficulty, because, in a complete solution, $\overline{\rho v}$ could be eliminated from the momentum and energy equations by the equation of continuity. An assumption for $\overline{\rho'v'}$ would be necessary only if it were desired to calculate $\bar{v}$.

APPENDIX B

PROOF THAT $\dfrac{\tau}{\tau_w} = \dfrac{q}{q_w}$ FOR $Pr = a = 1$

In terms of eddy diffusivities, the momentum and energy equations may be written as follows:

$$\bar{\rho}\bar{u}\,\frac{\partial \bar{u}}{\partial x} + \bar{\rho}\bar{v}\,\frac{\partial \bar{u}}{\partial y} = \frac{\partial}{\partial y}\left[(\bar{\mu} + \bar{\rho}\epsilon)\frac{\partial \bar{u}}{\partial y}\right] \tag{B1}$$

$$\bar{\rho}\bar{u}\,\frac{\partial}{\partial x}\left(c_p\bar{t} + \frac{\bar{u}^2}{2}\right) + \bar{\rho}\bar{v}\,\frac{\partial}{\partial y}\left(c_p\bar{t} + \frac{\bar{u}^2}{2}\right) = \frac{\partial}{\partial y}\left[(\bar{k} + \bar{\rho}c_p\epsilon_h)\frac{\partial \bar{t}}{\partial y} + \bar{u}(\bar{\mu} + \bar{\rho}\epsilon)\frac{\partial \bar{u}}{\partial y}\right]$$

$$\tag{B2}$$

The energy equation (B2) can be rearranged to read

$$\bar{\rho}\bar{u}\,\frac{\partial}{\partial x}\left(c_p\bar{t} + \frac{\bar{u}^2}{2}\right) + \bar{\rho}\bar{v}\,\frac{\partial}{\partial y}\left(c_p\bar{t} + \frac{\bar{u}^2}{2}\right)$$

$$= \frac{\partial}{\partial y}\left[\frac{\bar{\mu}}{Pr} + \bar{\rho}\epsilon_h\frac{\partial}{\partial y}(c_p\bar{t}) + (\bar{\mu} + \bar{\rho}\epsilon)\frac{\partial}{\partial y}\left(\frac{\bar{u}^2}{2}\right)\right] \tag{B3}$$

For $Pr = a = 1$, equation (B3) becomes

$$\bar{\rho}\bar{u}\,\frac{\partial}{\partial x}\left(c_p\bar{t} + \frac{\bar{u}^2}{2}\right) + \bar{\rho}\bar{v}\,\frac{\partial}{\partial y}\left(c_p\bar{t} + \frac{\bar{u}^2}{2}\right) = \frac{\partial}{\partial y}\left[(\bar{\mu} + \bar{\rho}\epsilon)\frac{\partial}{\partial y}\left(c_p\bar{t} + \frac{\bar{u}^2}{2}\right)\right] \tag{B4}$$

If equations (B1) and (B4) are each solved for $\bar{\rho}\bar{u}$ and the results equated, there is obtained

$$\frac{\dfrac{\partial}{\partial y}\left[(\bar{\mu} + \bar{\rho}\epsilon)\dfrac{\partial \bar{u}}{\partial y}\right] - \bar{\rho}\bar{v}\dfrac{\partial \bar{u}}{\partial y}}{\dfrac{\partial \bar{u}}{\partial x}} = \frac{\dfrac{\partial}{\partial y}\left[(\bar{\mu} + \bar{\rho}\epsilon)\dfrac{\partial}{\partial y}\left(c_p\bar{t} + \dfrac{\bar{u}^2}{2}\right)\right] - \bar{\rho}\bar{v}\dfrac{\partial}{\partial y}\left(c_p\bar{t} + \dfrac{\bar{u}^2}{2}\right)}{\dfrac{\partial}{\partial x}\left(c_p\bar{t} + \dfrac{\bar{u}^2}{2}\right)}$$

$$\tag{B5}$$

The assumption is now made that

$$c_p\bar{t} + \frac{\bar{u}^2}{2} = A\bar{u} + B \tag{B6}$$

The expression given by equation (B6) for $c_p\bar{t} + \dfrac{\bar{u}^2}{2}$ is substituted into the right side of equation (B5). Since the right side becomes identical with the left side upon this substitution, equation (B6) is a valid relation.

The constants A and B in equation (B6) are evaluated as follows:

at $y = 0$:

$$\bar{u} = 0, \quad \bar{t} = \bar{t}_w, \quad B = c_p \bar{t}_w$$

at $y = 0$:

$$\bar{\mu} \frac{\partial \bar{u}}{\partial y} = \tau_w, \quad -\bar{k} \frac{\partial \bar{t}}{\partial y} = q_w, \quad A = -\frac{q_w}{\tau_w}$$

With the constants thus evaluated, equation (B6) becomes (dropping the bars for convenience)

$$c_p t + \frac{u^2}{2} = -\frac{q_w}{\tau_w} u + c_p t_w \tag{B7}$$

If equation (B7) is made dimensionless, it becomes simply

$$u^+ = T^+ \tag{B8}$$

Previously obtained relations for τ/τ_w and q/q_w are

$$\frac{\tau}{\tau_w} = \left(\frac{\mu}{\mu_w} + \frac{\rho}{\rho_w} \frac{\epsilon}{\mu_w/\rho_w} \right) \frac{du^+}{dy^+} \tag{5}$$

$$\frac{q}{q_w} = \left(\frac{k}{k_w} \frac{1}{Pr_w} + \frac{\rho}{\rho_w} a \frac{\epsilon}{\mu_w/\rho_w} \right) \frac{dt^+}{dy^+} - 2 \frac{\alpha}{\beta} u^+ \left(\frac{\mu}{\mu_w} + \frac{\rho}{\rho_w} \frac{\epsilon}{\mu_w/\rho_w} \right) \frac{du^+}{dy^+} \tag{6}$$

If use is made of equations (B8), (10), and (26) and the fact that $Pr = a = 1$, the resulting equation can be reduced to

$$\frac{q}{q_w} = \frac{\tau}{\tau_w} \tag{B9}$$

APPENDIX C

VELOCITY AND TEMPERATURE PROFILES FOR CONSTANT RATIO OF TURBULENT

TO MOLECULAR SHEAR STRESS AT y_1^+ AND MOLECULAR SHEAR STRESS

AND HEAT TRANSFER IN REGION AWAY FROM WALL (Pr = 1)

The equation for velocity profile used near the wall is equation (16), where $1 - \alpha t^{+'} = 1 - \alpha u^{+2}$ for $Pr = 1$ and $\beta = 0$ (see eqs. (B8), (26), and definitions of t^+ and $t^{+'}$).

Previously, the expression for τ/τ_w was shown to be

$$\frac{\tau}{\tau_w} = \frac{\mu}{\mu_w} \frac{du^+}{dy^+} + \frac{\rho}{\rho_w} \frac{\epsilon}{\mu_w/\rho_w} \frac{du^+}{dy^+} \tag{5}$$

and far from the wall (eq. (8)),

$$\frac{\epsilon}{\mu_w/\rho_w} = \frac{\varkappa^2 \left(\dfrac{du^+}{dy^+}\right)^3}{\left(\dfrac{d^2 u^+}{dy^{+2}}\right)^2}$$

Combining equations (5) and (8) and assuming constant shear stress across the boundary layer give

$$1 = \left[\frac{\mu}{\mu_w} + \varkappa^2 \frac{\rho}{\rho_w} \frac{\left(\dfrac{du^+}{dy^+}\right)^3}{\left(\dfrac{d^2 u^+}{dy^{+2}}\right)^2} \right] \frac{du^+}{dy^+} \tag{C1}$$

The variations of density and viscosity with temperature are

$$\left. \begin{aligned} \frac{\mu}{\mu_w} &= \left(\frac{t}{t_w}\right)^{0.68} \\[2mm] \frac{\rho}{\rho_w} &= \frac{t_w}{t} \end{aligned} \right\} \tag{C2}$$

For $Pr = a = 1$ and $\beta = 0$, the temperature ratio is expressed as

$$\frac{t}{t_w} = 1 - \alpha u^{+2} \tag{C3}$$

Substitution of equations (C2) and (C3) into (C1) yields

$$1 = \left[(1 - \alpha u^{+2})^{0.68} + \frac{\varkappa^2}{1 - \alpha u^{+2}} \frac{\left(\dfrac{du^+}{dy^+}\right)^3}{\left(\dfrac{d^2u^+}{dy^{+2}}\right)^2} \right] \frac{du^+}{dy^+} \tag{C4}$$

Solving for d^2u^+/dy^{+2} gives

$$\frac{d^2u^+}{dy^{+2}} = \frac{-\varkappa \left(\dfrac{du^+}{dy^+}\right)^2}{\sqrt{(1 - \alpha u^{+2}) \left[1 - (1 - \alpha u^{+2})^{0.68} \dfrac{du^+}{dy^+} \right]}} \tag{C5}$$

If a change in variables is made as

$$v = \frac{du^+}{dy^+}$$

equation (C5) can be integrated to give

$$v = v_1 \, e^{-\displaystyle\int_{u_1^+}^{u^+} \frac{\varkappa\, du^+}{\sqrt{(1 - \alpha u^{+2})\left[1 - (1 - \alpha u^{+2})^{0.68} v\right]}}} \tag{C6}$$

The solutions for u^+ as a function of y^+ can be obtained by a process of iteration. Assumed values of v for a given increment in u^+ are substituted into the right side of equation (C6) until it equals the left side. The relation between u^+ and y^+ is then calculated from

$$y^+ = \int_0^{u^+} \frac{du^+}{v} \tag{C7}$$

From equation (B8), $u^+ = T^+$ for $q/q_w = \tau/\tau_w$, so that the relation between T^+ and y^+ is also known.

APPENDIX D

VELOCITY PROFILES FOR LINEAR VARIATION OF SHEAR STRESS

AND HEAT TRANSFER ACROSS BOUNDARY LAYER (Pr = 1)

Because the variation of shear in the thin region near the wall is negligible, the same equations are used in the present case as were used in appendix C.

From equation (5), the equation for τ/τ_w far from the wall, neglecting the viscous stress, is

$$\frac{\tau}{\tau_w} = \frac{\rho}{\rho_w} \frac{\epsilon}{\mu_w/\rho_w} \frac{du^+}{dy^+}$$

The expression for $\epsilon/(\mu_w/\rho_w)$ far from the wall is, from equation (8),

$$\frac{\epsilon}{\mu_w/\rho_w} = \frac{\varkappa^2 \left(\dfrac{du^+}{dy^+}\right)^3}{\left(\dfrac{d^2 u^+}{dy^{+2}}\right)^2}$$

For a linear variation in shear stress,

$$\frac{\tau}{\tau_w} = 1 - \frac{y^+}{\delta^+} \tag{D1}$$

Combining the foregoing equations yields

$$1 - \frac{y^+}{\delta^+} = \frac{\rho}{\rho_w} \frac{\varkappa^2 \left(\dfrac{du^+}{dy^+}\right)^4}{\left(\dfrac{d^2 u^+}{dy^{+2}}\right)^2} \tag{D2}$$

For $\beta = 0$, $Pr = a = 1$ $(\tau/\tau_w = q/q_w)$,

$$\frac{t}{t_w} = 1 - \alpha u^{+2} = \frac{\rho_w}{\rho} \tag{D3}$$

Substituting equation (D3) into (D2), rearranging, and taking the square
root of both sides give

$$\frac{d^2 u^+}{dy^{+2}} = \frac{-\varkappa}{\sqrt{1 - \alpha u^{+2}}} \frac{\left(\dfrac{du^+}{dy^+}\right)^2}{\sqrt{1 - \dfrac{y^+}{\delta^+}}} \tag{D4}$$

Letting $v = du^+/dy^+$ in equation (D4) and integrating give

$$v = v_1 \, e^{\displaystyle -\varkappa \int_{u_1^+}^{u^+} \frac{du^+}{\sqrt{1-\alpha u^{+2}}\,\sqrt{1 - \dfrac{y_1^+}{\delta^+} - \dfrac{1}{\delta^+}\displaystyle\int_{u_1^+}^{u^+}\dfrac{du^+}{v}}}} \tag{D5}$$

Equation (D5) can be solved by iteration for $\beta = 0$ and a given α and
δ^+, to give u^+ as a function of y^+. From equation (B8), $u^+ = T^+$ for
$q/q_w = \tau/\tau_w$, so that the relation between T^+ and y^+ is also known.

<div align="center">REFERENCES</div>

1. Rubesin, Morris W., Maydew, Randall C., and Varga, Steven A.: An
   Analytical and Experimental Investigation of the Skin Friction of
   the Turbulent Boundary Layer on a Flat Plate at Supersonic Speeds.
   NACA TN 2305, 1951.

2. Coles, Donald: Measurements in the Boundary Layer on a Smooth Flat
   Plate in Supersonic Flow. III - Measurements in a Flat-Plate
   Boundary Layer at the Jet Propulsion Laboratory. Rep. No. 20-71,
   Jet Prop. Lab., C.I.T., June 1, 1953. (Contract No. DA-04-495-ORD
   18, Dept. Army, Ord. Corps.)

3. Eckert, Ernst R. G.: Survey on Heat Transfer at High Speeds. Tech.
   Rep. 54-70, Aero. Res. Lab., WADC, Apr. 1954. (Contract No. AF
   33(616)-2214.)

4. Deissler, Robert G.: Analytical and Experimental Investigation of
   Adiabatic Turbulent Flow in Smooth Tubes. NACA TN 2138, 1950.

5. Deissler, R. G.: Investigation of Turbulent Flow and Heat Transfer
   in Smooth Tubes, Including the Effects of Variable Fluid Properties.
   Trans. ASME, vol. 73, no. 2, Feb. 1951, pp. 101-107.

4616

CN-5 back

6. Deissler, R. G.: Heat Transfer and Fluid Friction for Fully Developed Turbulent Flow of Air and Supercritical Water with Variable Fluid Properties. Trans. ASME, vol. 76, no. 1, Jan. 1954, pp. 73-85.

7. von Kármán, Th.: Turbulence and Skin Friction. Jour. Aero. Sci., vol. 1, no. 1, Jan. 1934, pp. 1-20.

8. Deissler, R. G., and Eian, C. S.: Analytical and Experimental Investigation of Fully Developed Turbulent Flow of Air in a Smooth Tube with Heat Transfer with Variable Fluid Properties. NACA TN 2629, 1952.

9. Deissler, Robert G.: Turbulent Heat Transfer and Friction in the Entrance Regions of Smooth Passages. Trans. ASME, vol. 77, no. 8, Nov. 1955, pp. 1221-1232; discussion, p. 1233.

10. Deissler, Robert G.: Analysis of Turbulent Heat Transfer, Mass Transfer, and Friction in Smooth Tubes at High Prandtl and Schmidt Numbers. NACA Rep. 1210, 1955. (Supersedes NACA TN 3145.)

11. Deissler, R. G., and Loeffler, A. L., Jr.: Turbulent Flow and Heat Transfer on a Flat Plate at High Mach Number with Variable Fluid Properties. Paper No. 55-A-133, ASME, 1955.

12. Reichardt, H.: Fundamentals of Turbulent Heat Transfer. Archiv f. d. gesamte Wärmetech., no. 6/7, 1951, pp. 129-142.

13. Goldstein, S., ed.: Modern Developments in Fluid Dynamics. Vol. II. Clarendon Press (Oxford), 1938, p. 351.

14. Laufer, John: The Structure of Turbulence in Fully Developed Pipe Flow. NACA Rep. 1174, 1954. (Supersedes NACA TN 2954.)

15. Klebanoff, P. S.: Characteristics of Turbulence in a Boundary Layer with Zero Pressure Gradient. NACA Rep. 1247, 1955. (Supersedes NACA TN 3178.)

16. von Kármán, Th.: The Problem of Resistance in Compressible Fluids. Reale Accad. d'Italia (Rome), T. XIII, Sept.-Oct. 1935.

17. Monaghan, R. J., and Cooke, J. R.: The Measurement of Heat Transfer and Skin Friction at Supersonic Speeds. Pt. IV. Tests on a Flat Plate at M = 2.82. Tech. Note AERO. 2171, British RAE, June 1952.

18. Hill, F. K.: Boundary-Layer Measurements in Hypersonic Flow. Jour. Aero. Sci., vol. 23, no. 3, Jan. 1956, pp. 35-42.

19. Rubesin, Morris W.: A Modified Reynolds Analogy for the Compressible
    Turbulent Boundary Layer on a Flat Plate. NACA TN 2917, 1953.

20. Crown, J. C.: The Laminar Boundary Layer at Hypersonic Speeds.
    NAVORD Rep. 2299, Naval Ord. Lab., Apr. 15, 1952.

21. Moore, L. L.: A Solution of·the Laminar Boundary-Layer Equations for
    a Compressible Fluid with Variable Properties, Including Dissocia-
    tion. Jour. Aero. Sci., vol. 19, no. 8, Aug. 1952, pp. 505-518.

22. Van Driest, E. R.: Turbulent Boundary Layer in Compressible Fluids.
    Jour. Aero. Sci., vol. 18, no. 3, Mar. 1951, pp. 145-161.

23. Lobb, R. Kenneth, Winkler, Eva M., and Persh, Jerome: Experimental
    Investigation of Turbulent Boundary Layers in Hypersonic Flow.
    Jour. Aero. Sci., vol. 22, no. 1, Jan. 1955, pp. 1-9; 50.

24. Brinich, Paul F., and Diaconis, Nick S.: Boundary-Layer Development
    and Skin Friction at Mach Number 3.05. NACA TN 2742, 1952.

25. Spivack, H. M.: Experiments in the Turbulent Boundary Layer of a
    Supersonic Flow. Rep. CM-615 (AL-1052), Aerophys. Lab., North Am.
    Aviation, Inc., Jan 16, 1950.

26. Monaghan, R. J., and Johnson, J. E.: The Measurement of Heat Trans-
    fer and Skin Friction at Supersonic Speeds. Pt. II. Boundary-
    Layer Measurements on a Flat Plate at M = 2.5 and Zero Heat Trans-
    fer. C. P. 64, British ARC, 1952.

27. Schultz-Grunow, F.: New Frictional Resistance Law for Smooth Plates.
    NACA TM 986, 1941.

28. Slack, Ellis G.: Experimental Investigation of Heat Transfer Through
    Laminar and Turbulent Boundary Layers on a Cooled Flat Plate at a
    Mach Number of 2.4. NACA TN 2686, 1952.

29. Pappas, C. C.: Measurement of Heat Transfer in the Turbulent Bound-
    ary Layer on a Flat Plate in Supersonic Flow and Comparison with
    Skin-Friction Results. NACA TN 3222, 1954.

30. Emmons, M. A., Jr., and Blanchard, R. F.: Preliminary Investigation
    of the Transfer of Heat from a Flat Plate at a Mach Number of 1.5.
    NACA RM L51H31, 1951.

31. Jacob, Max, and Dow, W. M.: Heat Transfer from a Cylindrical Surface
    to Air in Parallel Flow with and without Unheated Starting Sections.
    Trans. ASME, vol. 68, no. 2, Feb. 1946, pp. 123-134.

32. Dhawan, Satish: Direct Measurements of Skin Friction. NACA Rep.
    1121, 1953. (Supersedes NACA TN 2567.)

33. Kempf, Gunther: Neue Ergebnisse der Widerstandsforschung. Werft
    Reederei Hafen, Bd. 10, June 1929, pp. 234-239; 247-253.

4616

O Ref. 15 (flat plate)

$$u^+ = \frac{1}{\varkappa} \ln\left(\frac{y^+}{y_1^+}\right) + u_1^+$$

where

$\varkappa = 0.36$
$y_1^+ = 26.00$
$u_1^+ = 12.90$

$$y^+ = \frac{1}{n} \frac{\dfrac{1}{\sqrt{2\pi}} \displaystyle\int_0^{nu^+} e^{\frac{-(nu^+)^2}{2}} \, d(nu^+)}{\dfrac{1}{\sqrt{2\pi}} e^{\frac{-(nu^+)^2}{2}}}$$

where n = 0.109

Velocity parameter, u^+

Wall distance parameter, y^+
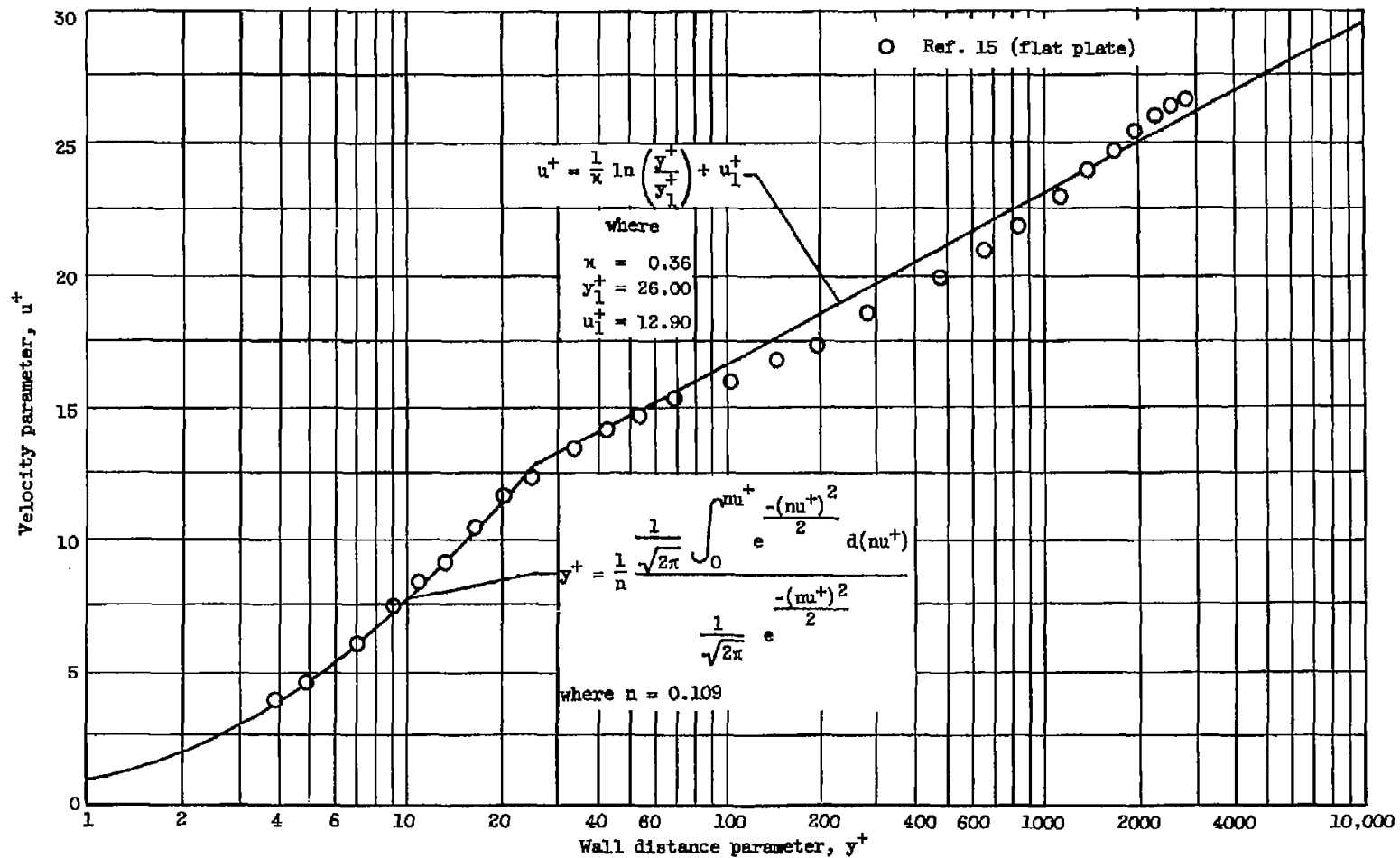
Figure 1. - Generalized computed velocity distribution for constant-property turbulent flow (ref. 4) with constants in
equations determined from pipe data compared with data for low-speed boundary-layer flow on a flat plate.
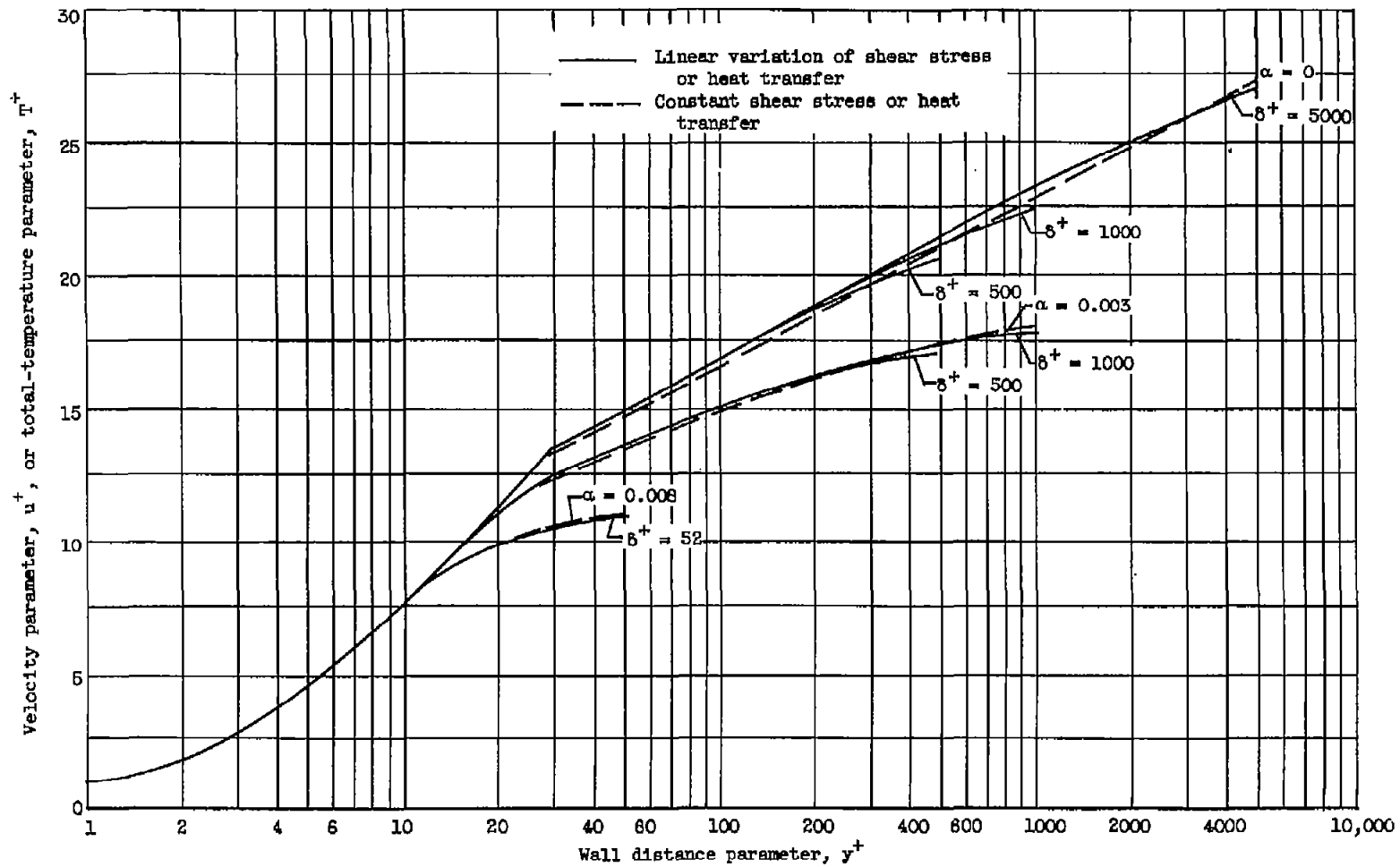
Figure 2. - Predicted effect of variation of shear stress and heat transfer across boundary layer on velocity and temperature distributions. Prandtl number, 1; heat-flux parameter β, 0.

Velocity parameter, u^+, or total-temperature parameter, τ^+

30

25

20

15

10

5

0

- - - - Constant y_1^+

———— y_1^+ at constant ratio of turbulent to viscous shear stress

Frictional-heating parameter, α

0

0.003

0.006

1   2   4   6   10   20   40   60   100   200   400   600   1000

Wall distance parameter, y^+
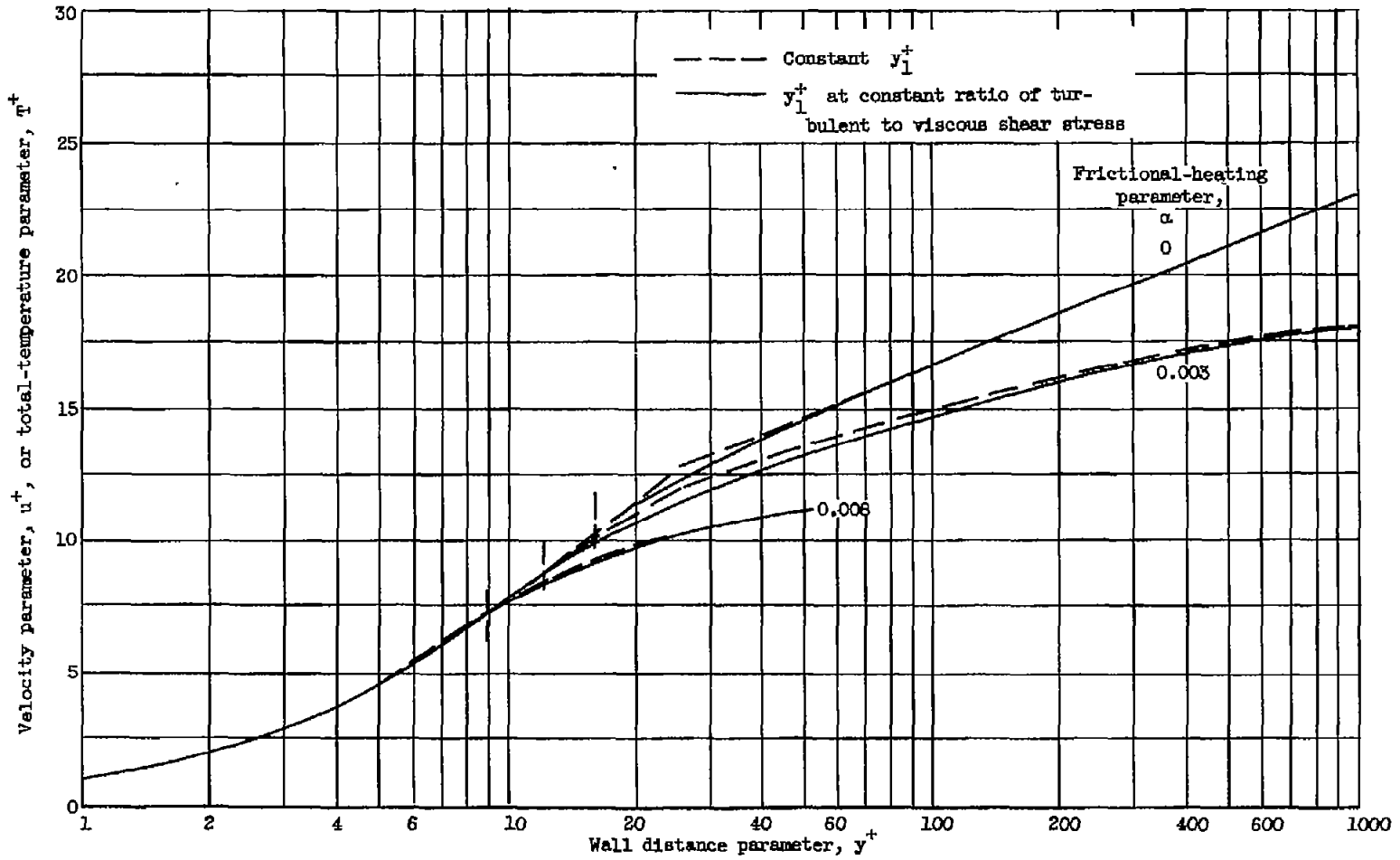
Figure 3. - Effect of various assumptions for variation of y_1^+ on generalized velocity or temperature distribution. Prandtl number, 1; heat-flux parameter β, 0.
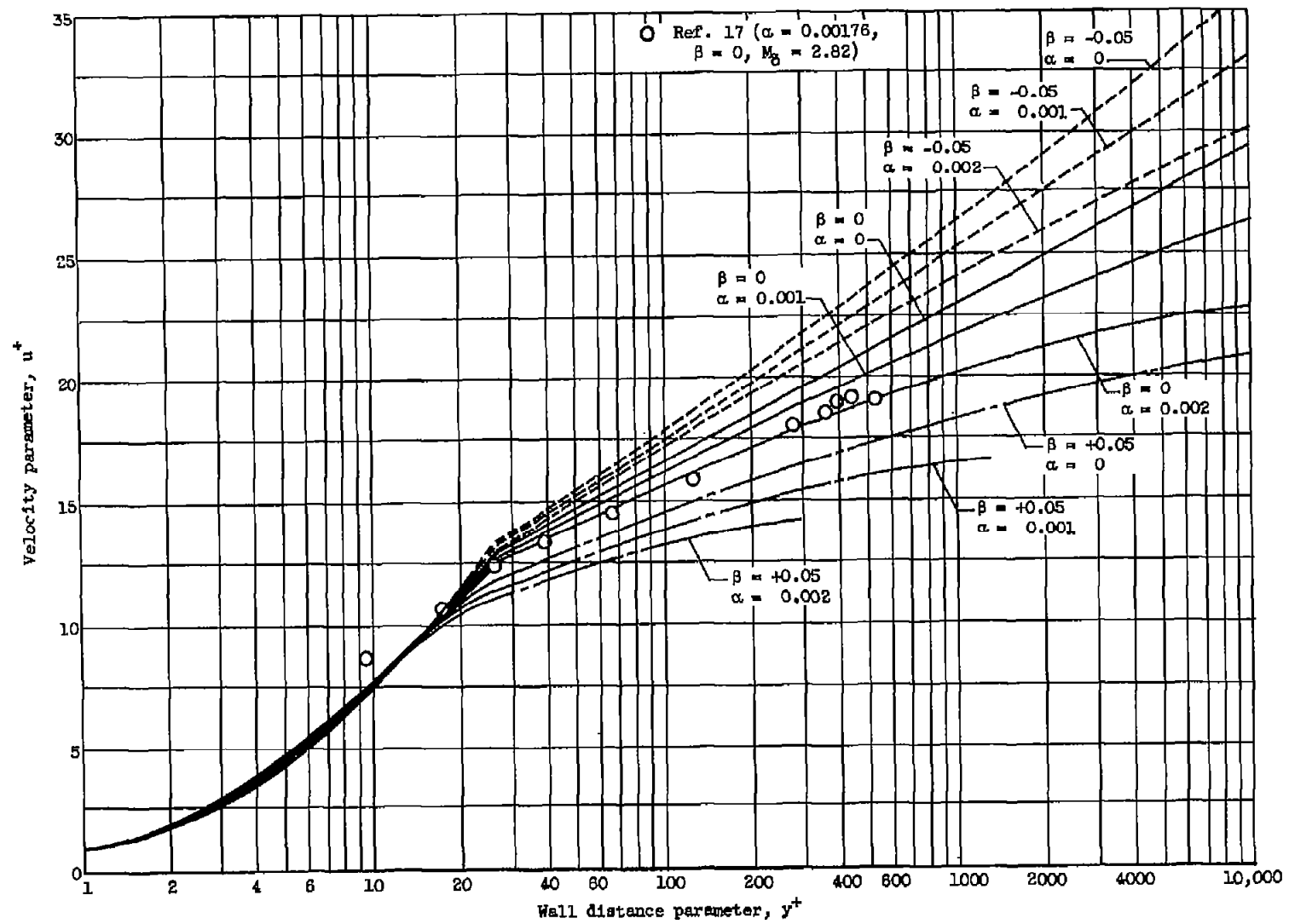
Figure 4. - Predicted generalized velocity distribution for air with heat transfer and frictional heating. Prandtl number, 0.73.
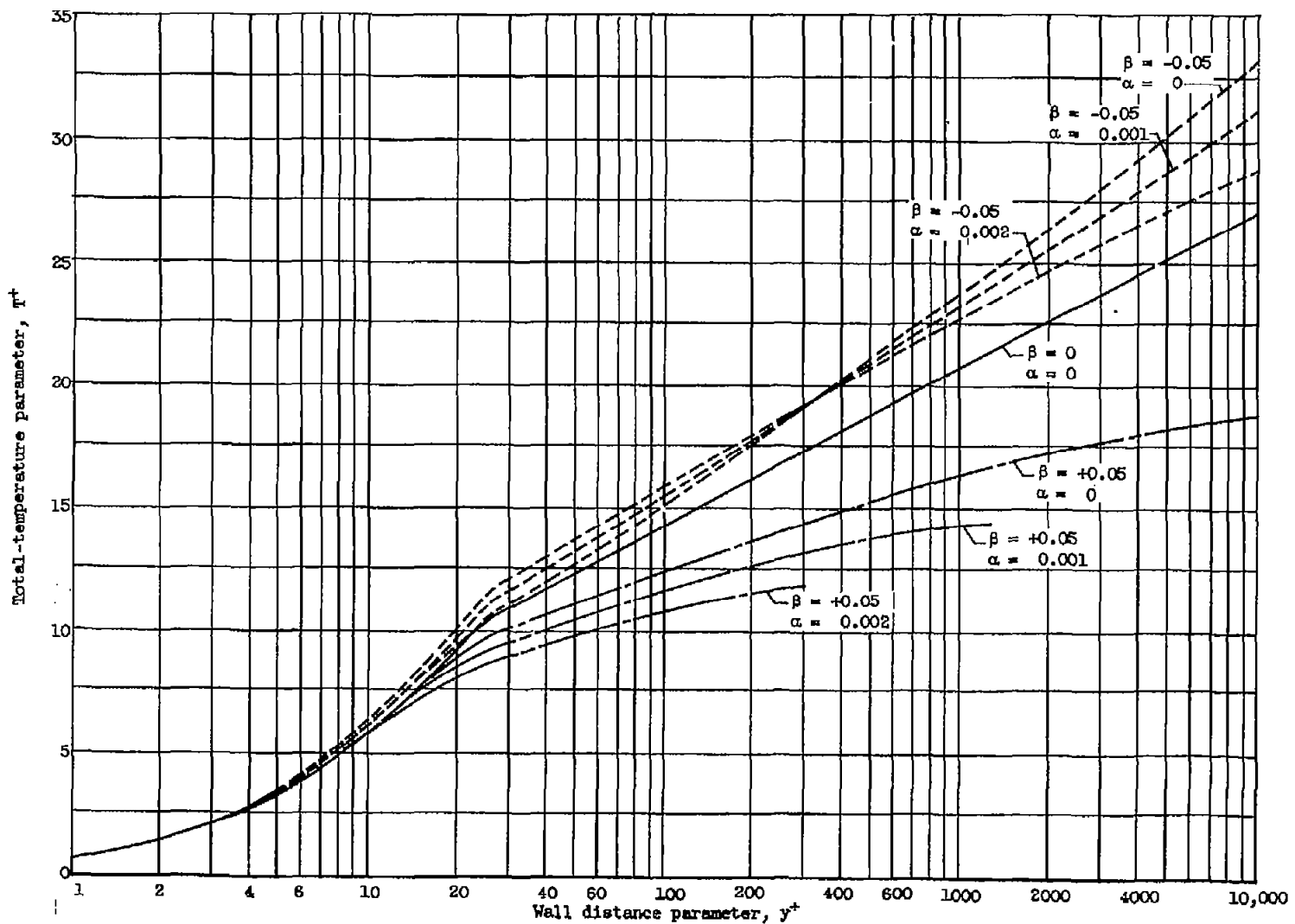
Figure 5. - Predicted generalized total-temperature distribution for air with heat transfer and frictional heating. Prandtl number, 0.73.
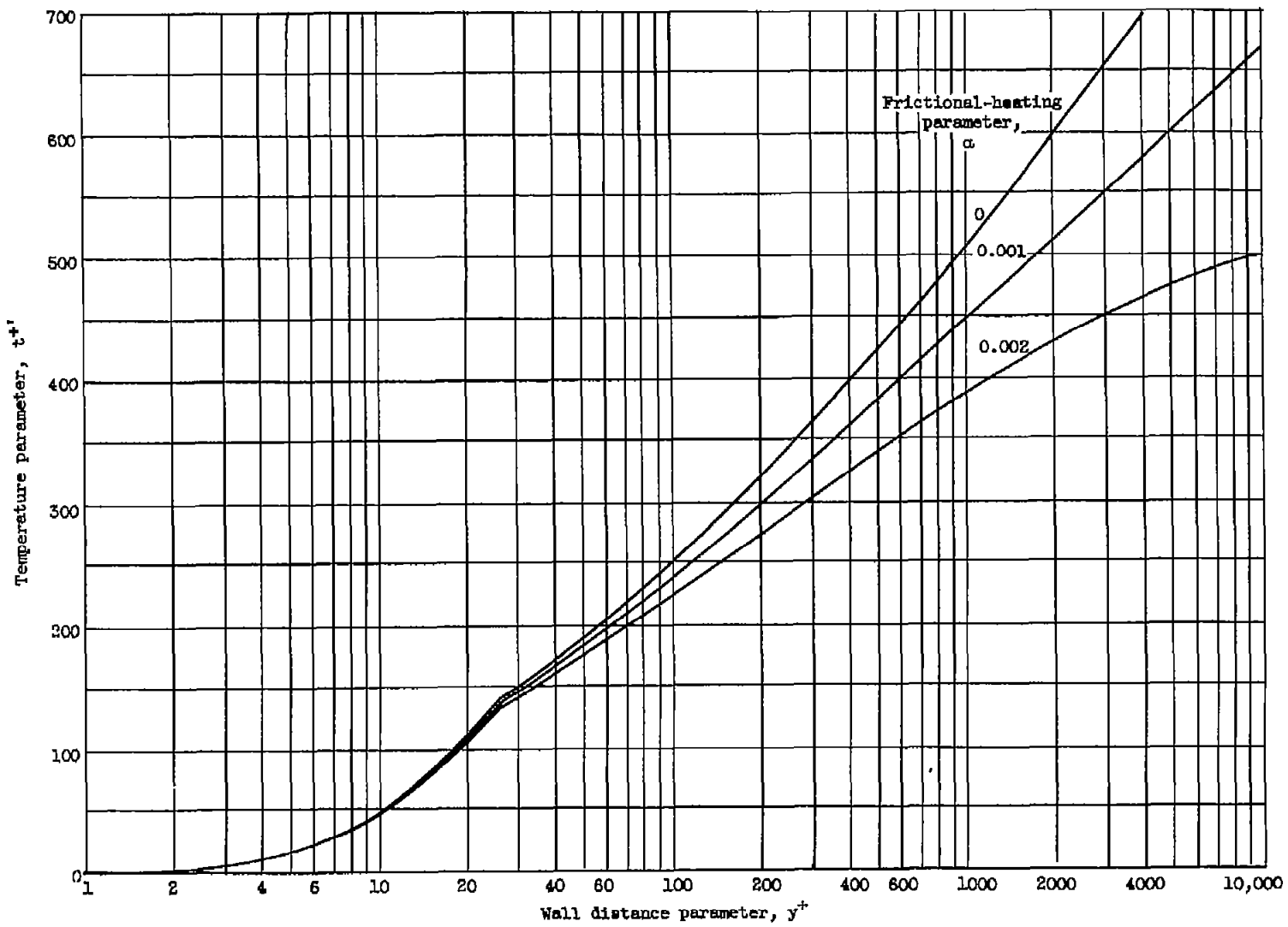
Figure 6. - Predicted temperature distribution for air with frictional heating on insulated plate. Prandtl number, 0.73.

Free-stream
Mach number,
M_δ

0
1
2
3
4
5
6
7
8
10
12
16
20

Skin-friction coefficient, C_f

10^{-2}

10^{-3}

10^{-4}

	Free-stream Mach number, M_δ	Reference
◁	4.93	23
◇	4.53	2
◊	3.70	2
△	3.05	24
○	2.82	17
▽	2.80	25
◊	2.58	2
◘	2.50	1
□	2.46	26
△	0	27

10^2 10^3 10^4 10^5

Momentum-thickness Reynolds number, Re_θ
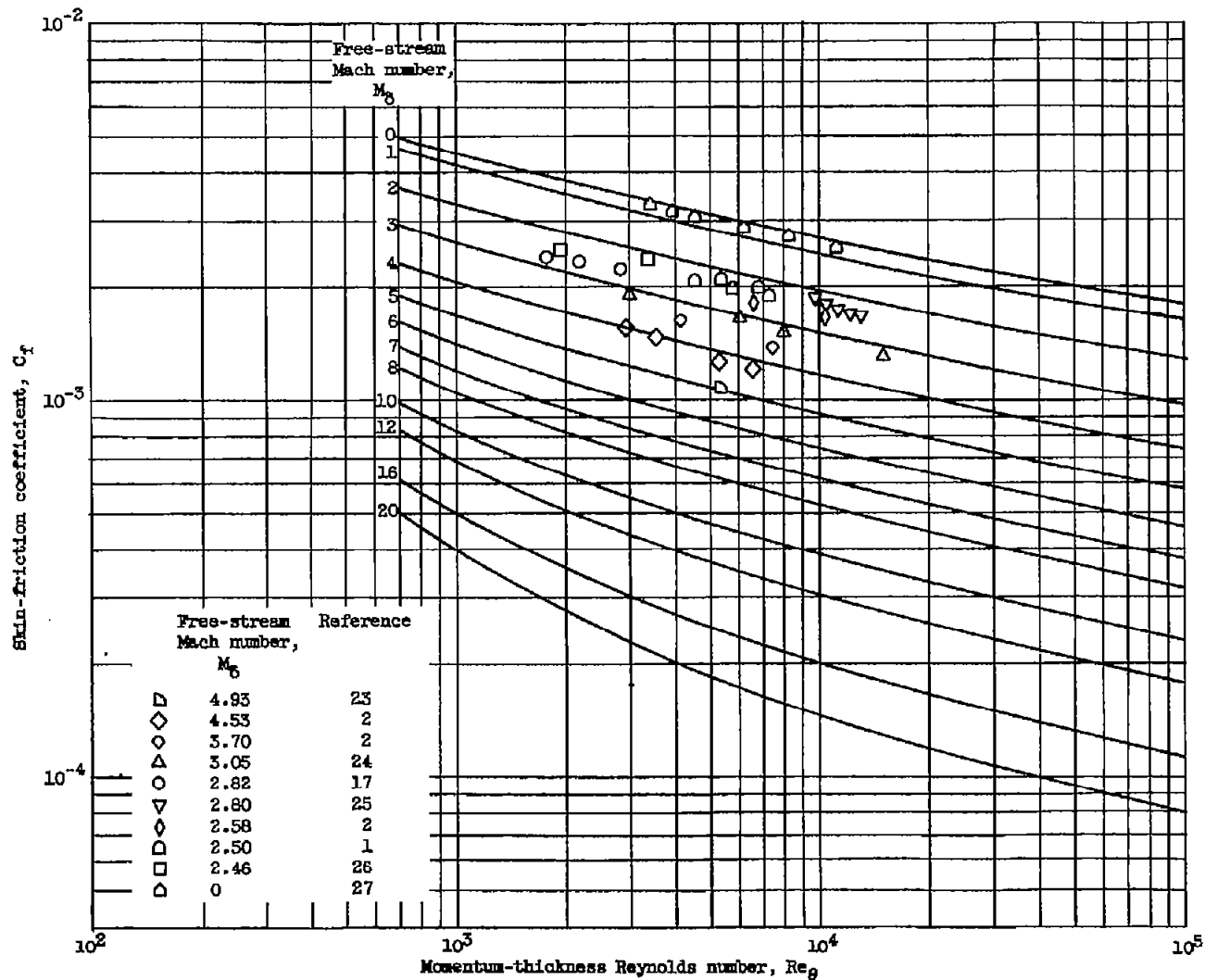
Figure 7. - Variation of predicted skin-friction coefficient with momentum-thickness Reynolds number and Mach number for insulated plate and comparison with experiment. Prandtl number, 0.73; heat-flux parameter β, 0.
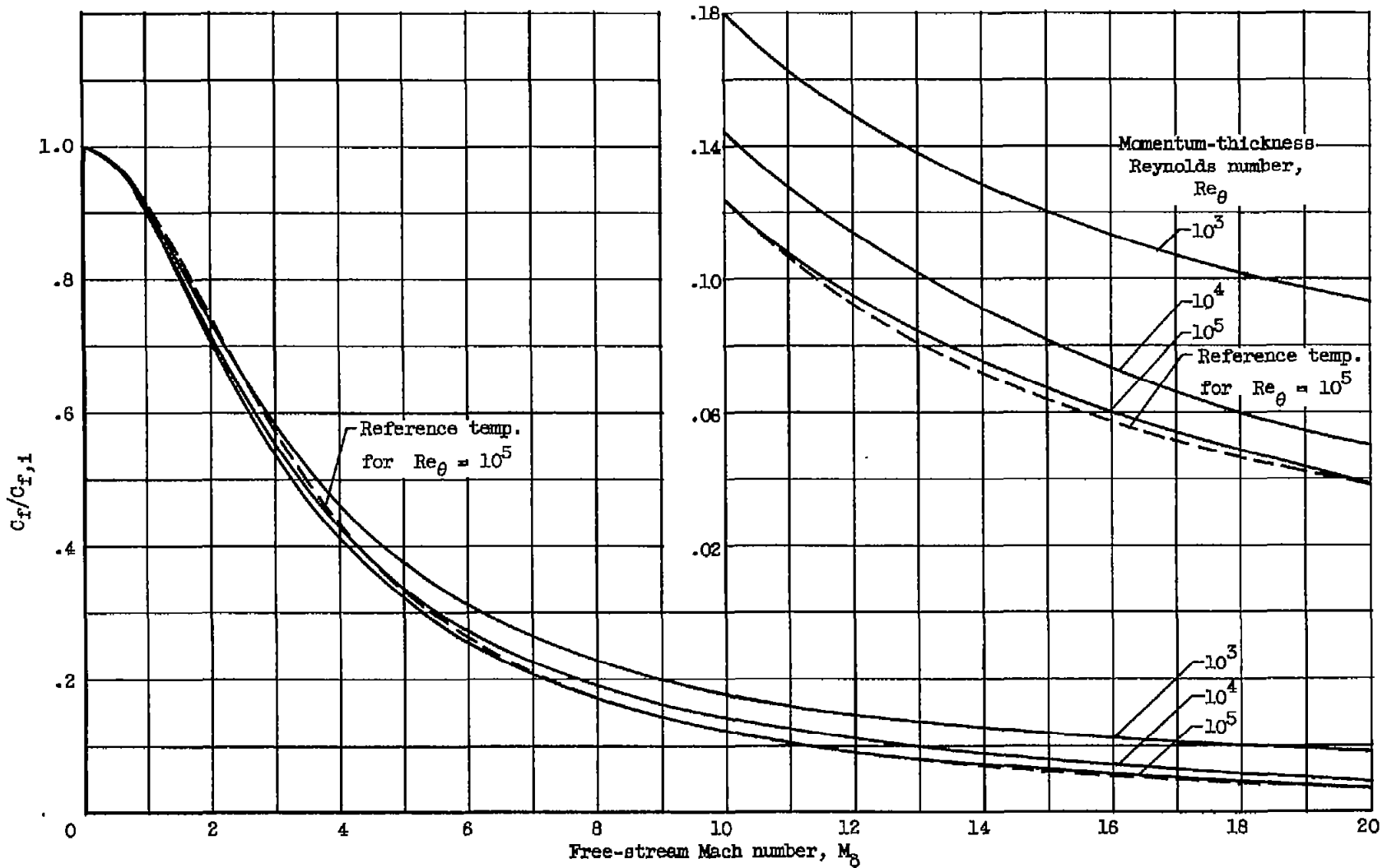
Figure 8. - Variation of $C_f/C_{f,i}$ with Mach number for various values of momentum-thickness Reynolds number for insulated plate. Prandtl number, 0.73; heat-flux parameter β, 0.
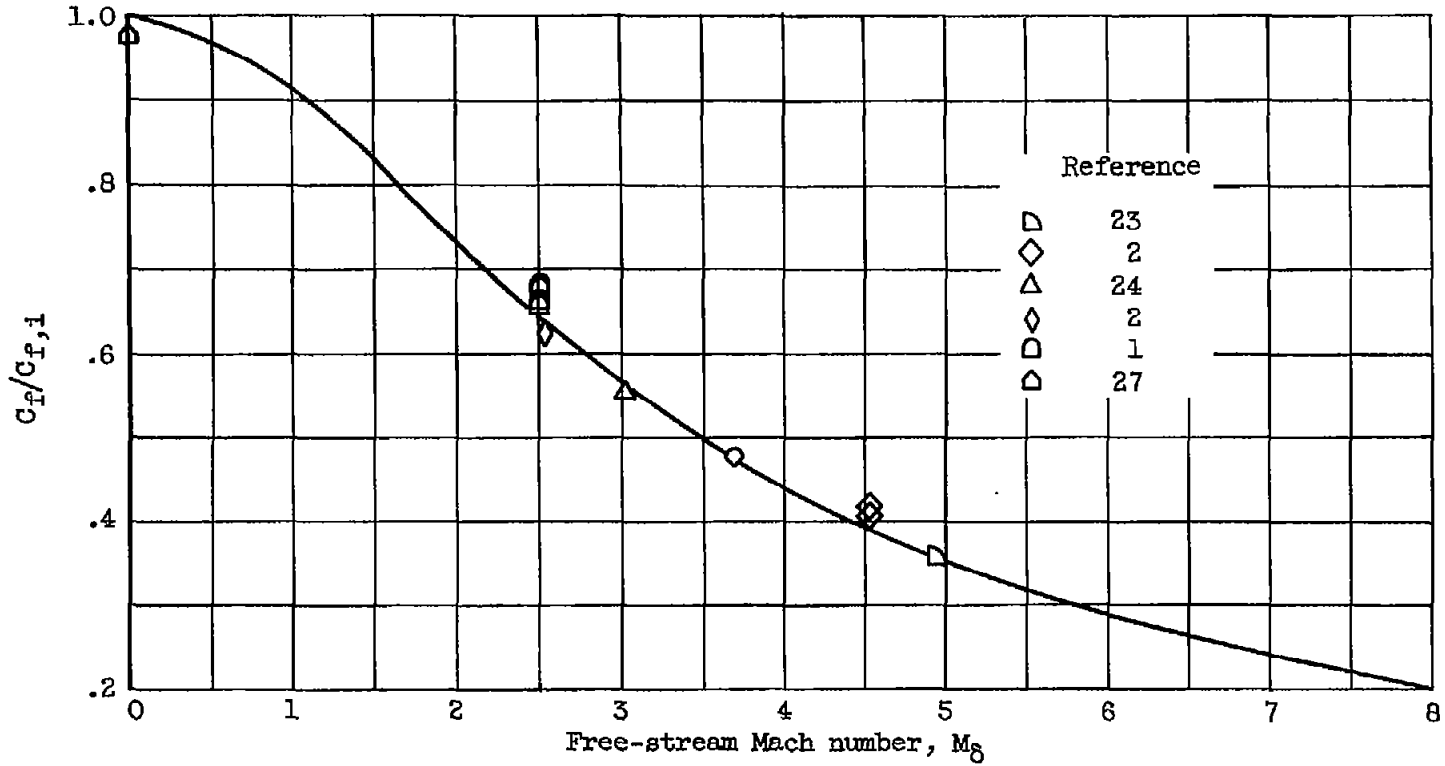
Figure 9. - Variation of $C_f/C_{f,i}$ with Mach number for momentum-thickness Reynolds number of 6000 for insulated plate and comparison with experiment. Prandtl number, 0.73; heat-flux parameter β, 0.
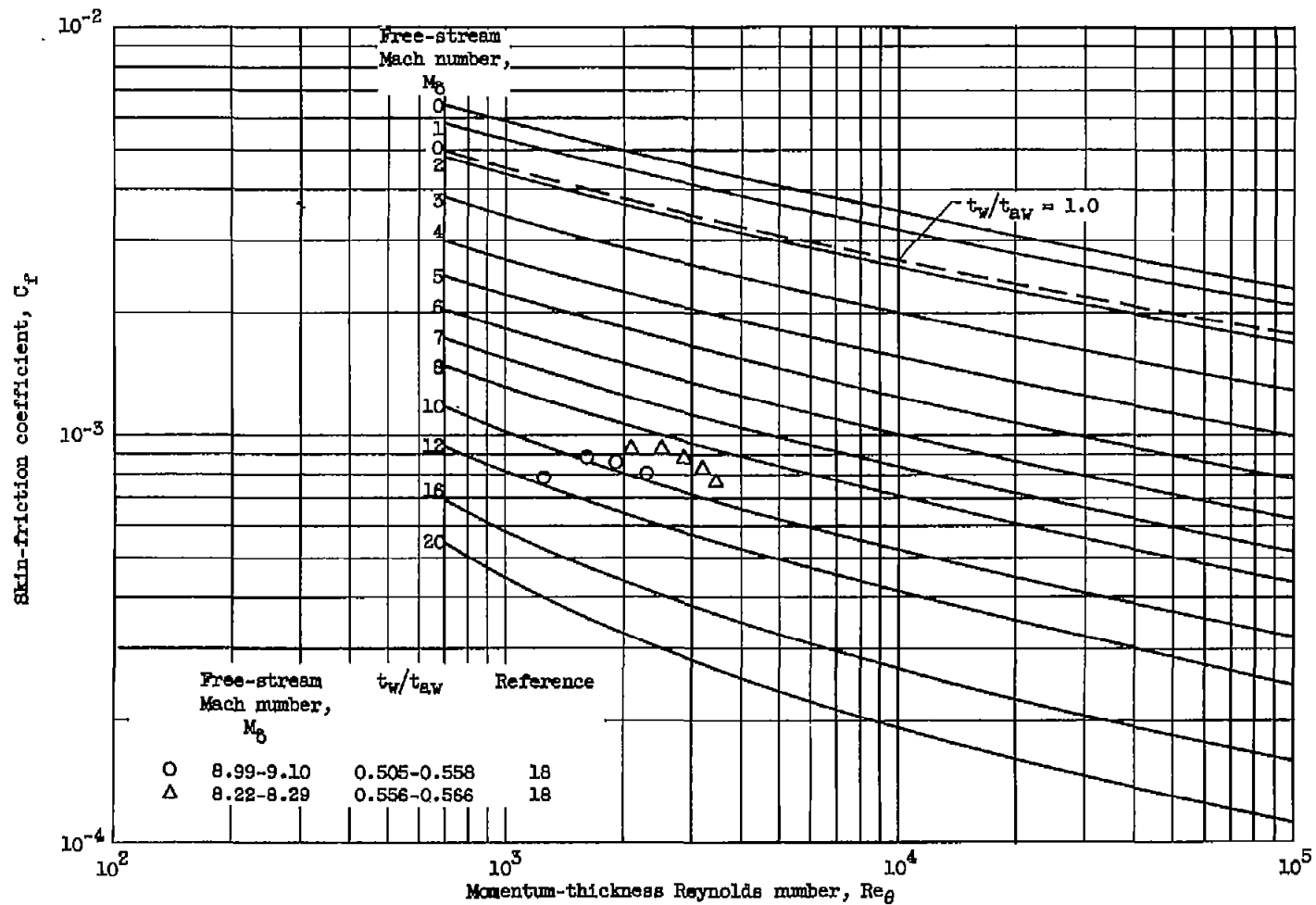
Figure 10. - Variation of predicted skin-friction coefficient with momentum-thickness Reynolds number and Mach number for t_w/t_{aw} of 0.5 and comparison with experiment. Prandtl number, 0.73.
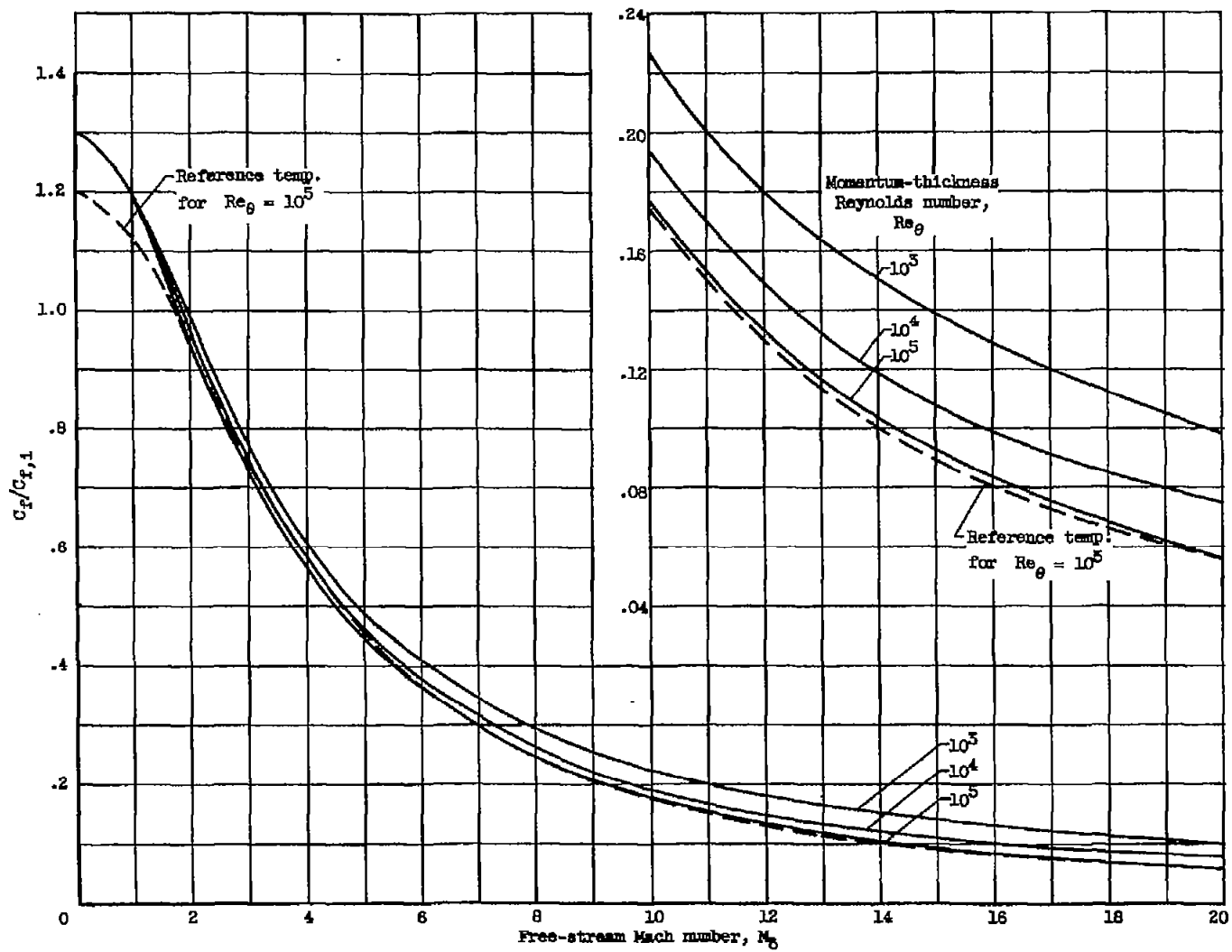
Figure 11. - Variation of $C_f/C_{f,i}$ with Mach number for various values of momentum-thickness Reynolds number and t_w/t_{aw} of 0.5. Prandtl number, 0.73.

Figure 12. - Variation of predicted Stanton number with momentum-thickness Reynolds number and Mach number for insulated plate and comparison with experiment. Prandtl number, 0.73.
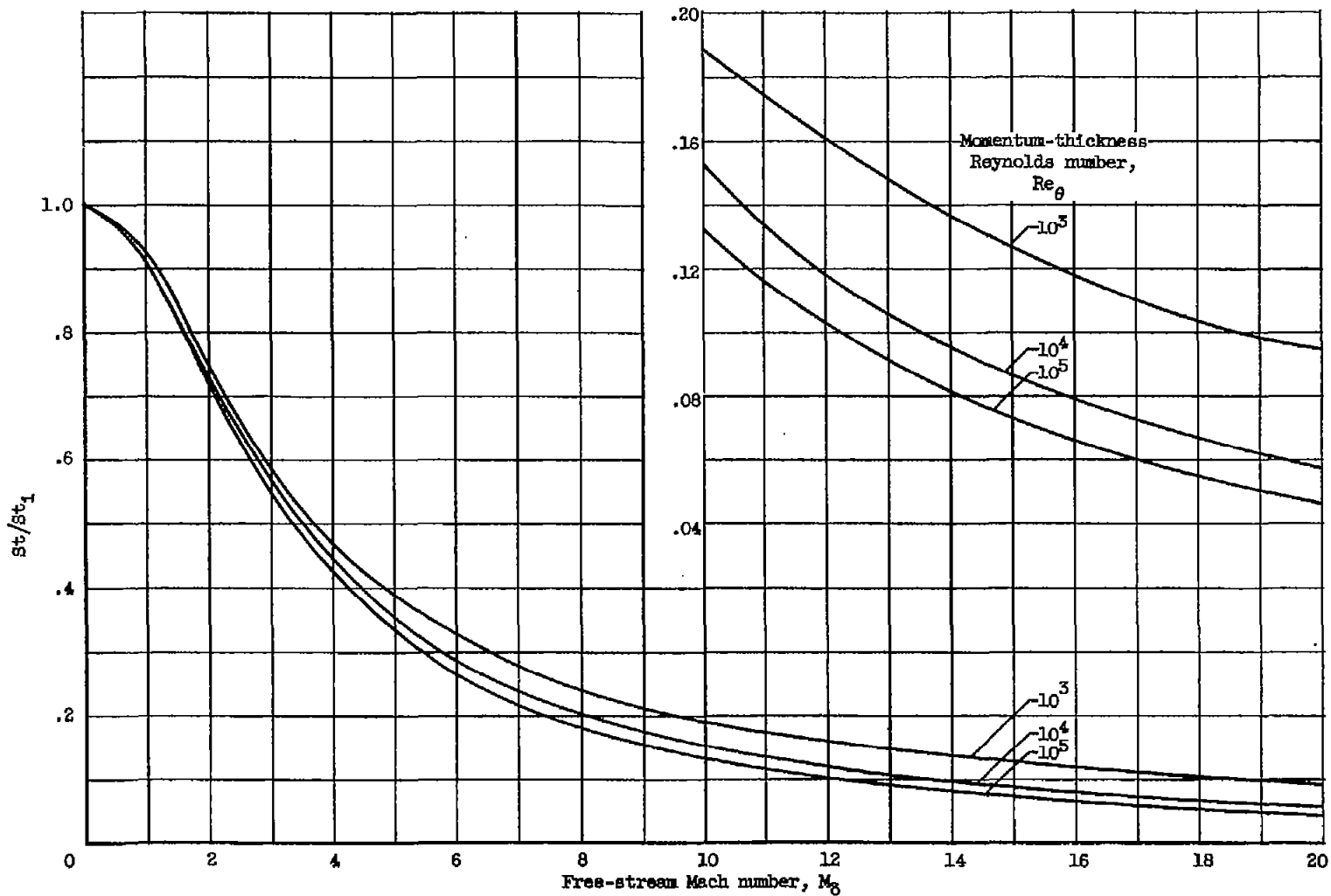
Figure 13. - Variation of St/St_1 with Mach number for various values of momentum-thickness Reynolds number for insulated plate. Prandtl number, 0.73; heat-flux parameter β, 0.
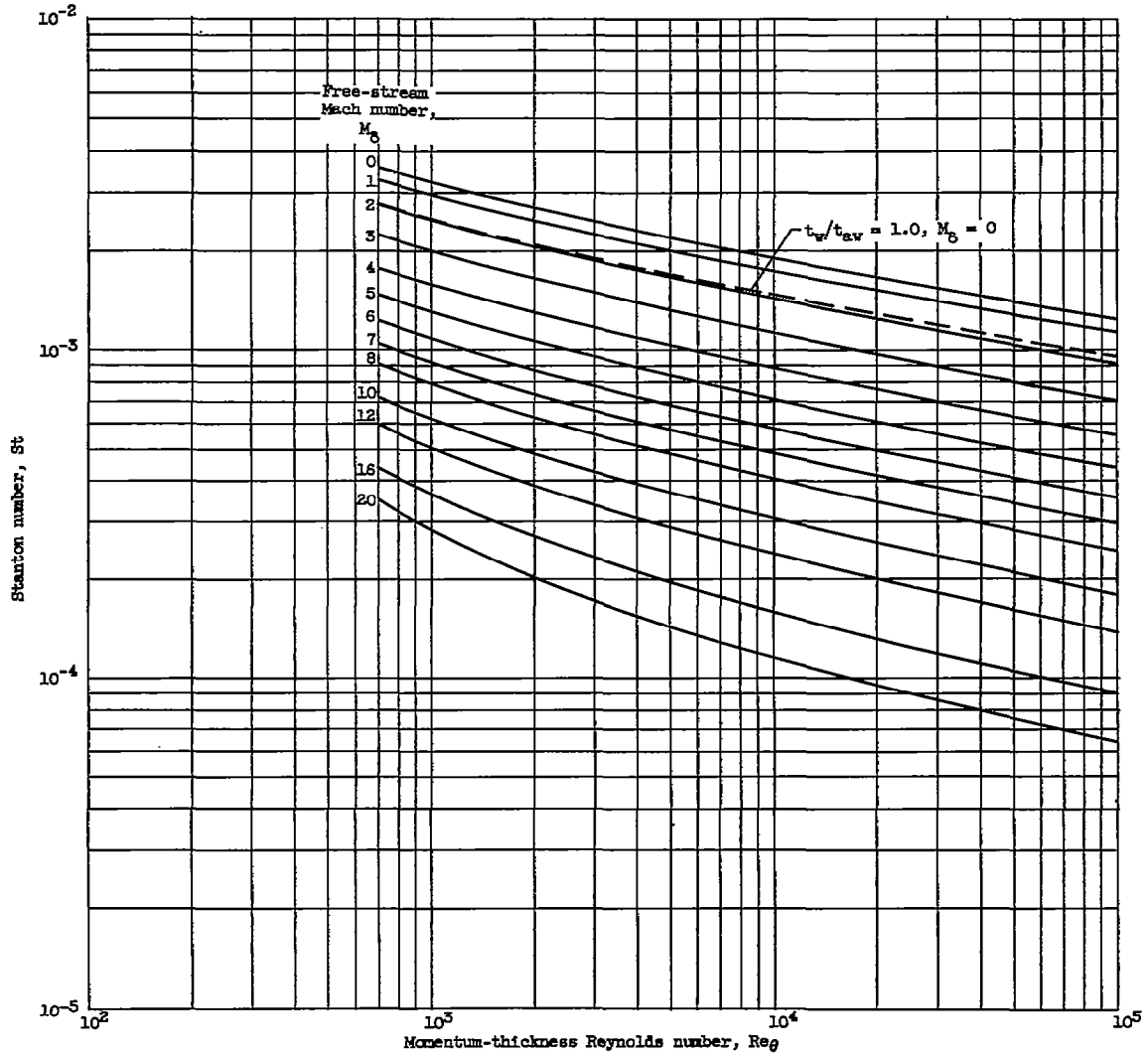
Figure 14. - Variation of predicted Stanton number with momentum-thickness Reynolds number and Mach number for t_w/t_{av} of 0.5. Prandtl number, 0.73.
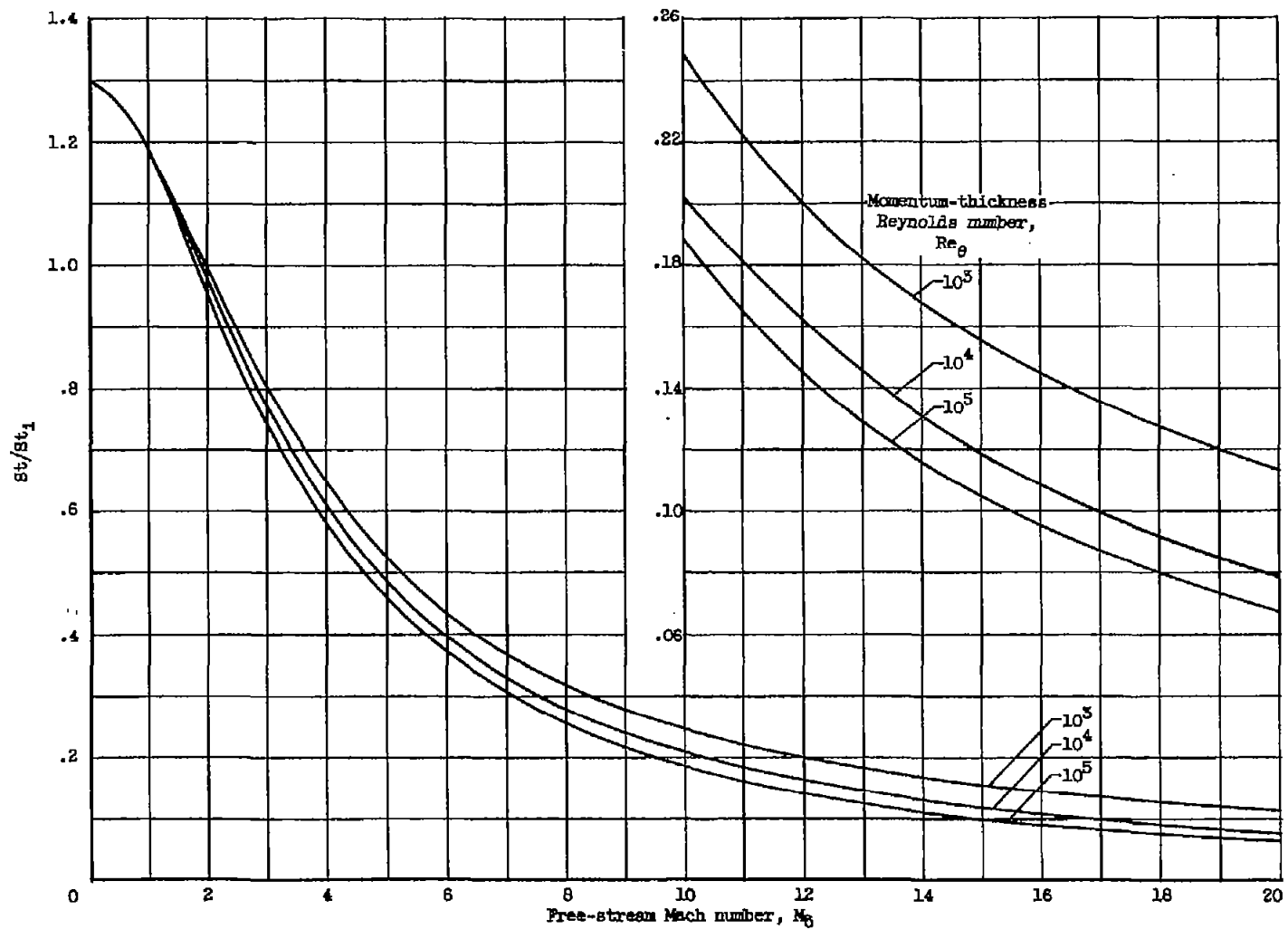
Figure 15. – Variation of St/St_1 with Mach number for various values of momentum-thickness Reynolds number and t_w/t_{aw} of 0.5. Prandtl number, 0.75.
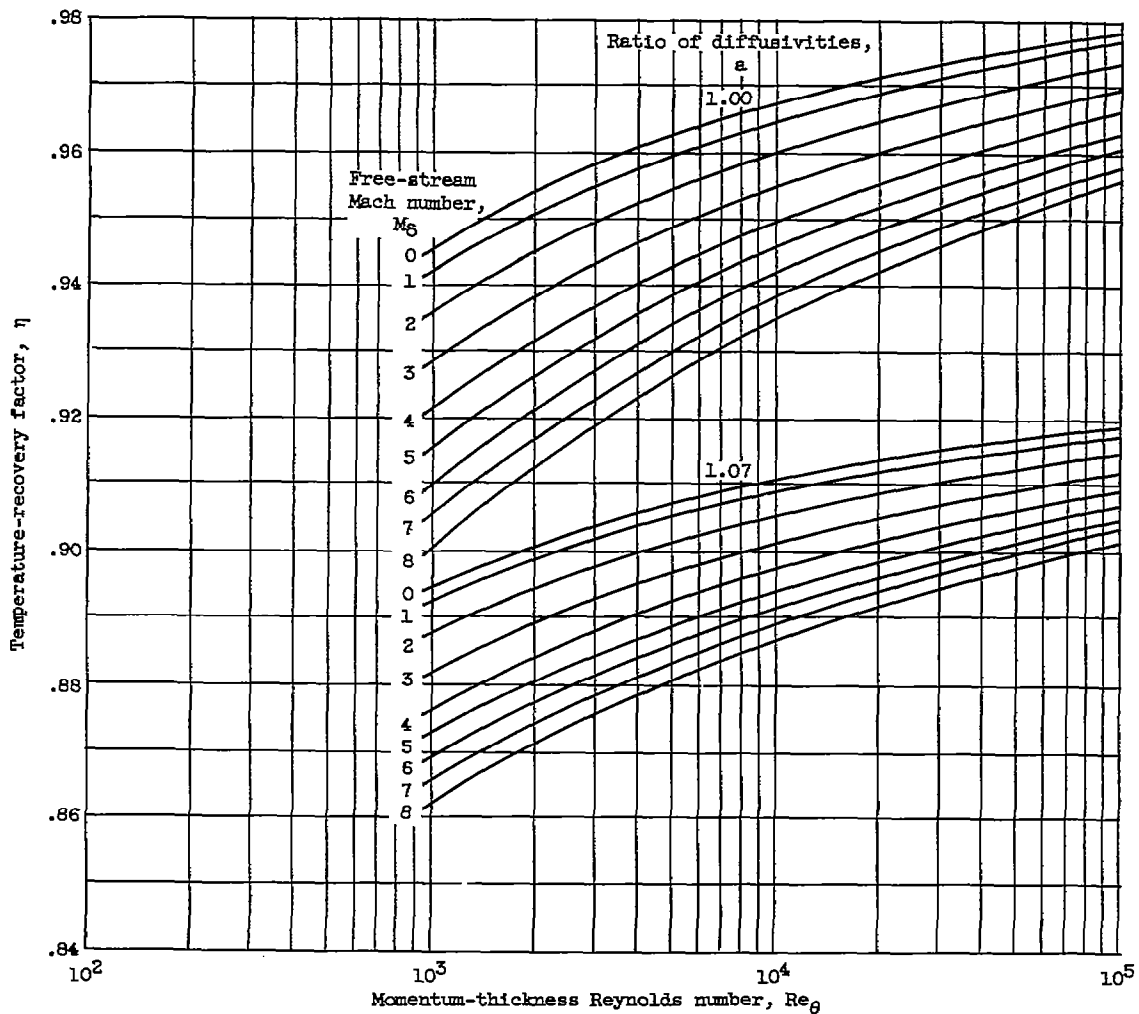
Figure 16. - Predicted variation of temperature-recovery factor with momentum-thickness
Reynolds number and Mach number for $\epsilon_h/\epsilon = a = 1$ and 1.07. Prandtl number, 0.73.

(a) Insulated plate. Heat-flux parameter β, 0.

(b) $t_w/t_{aw} = 0.5$.
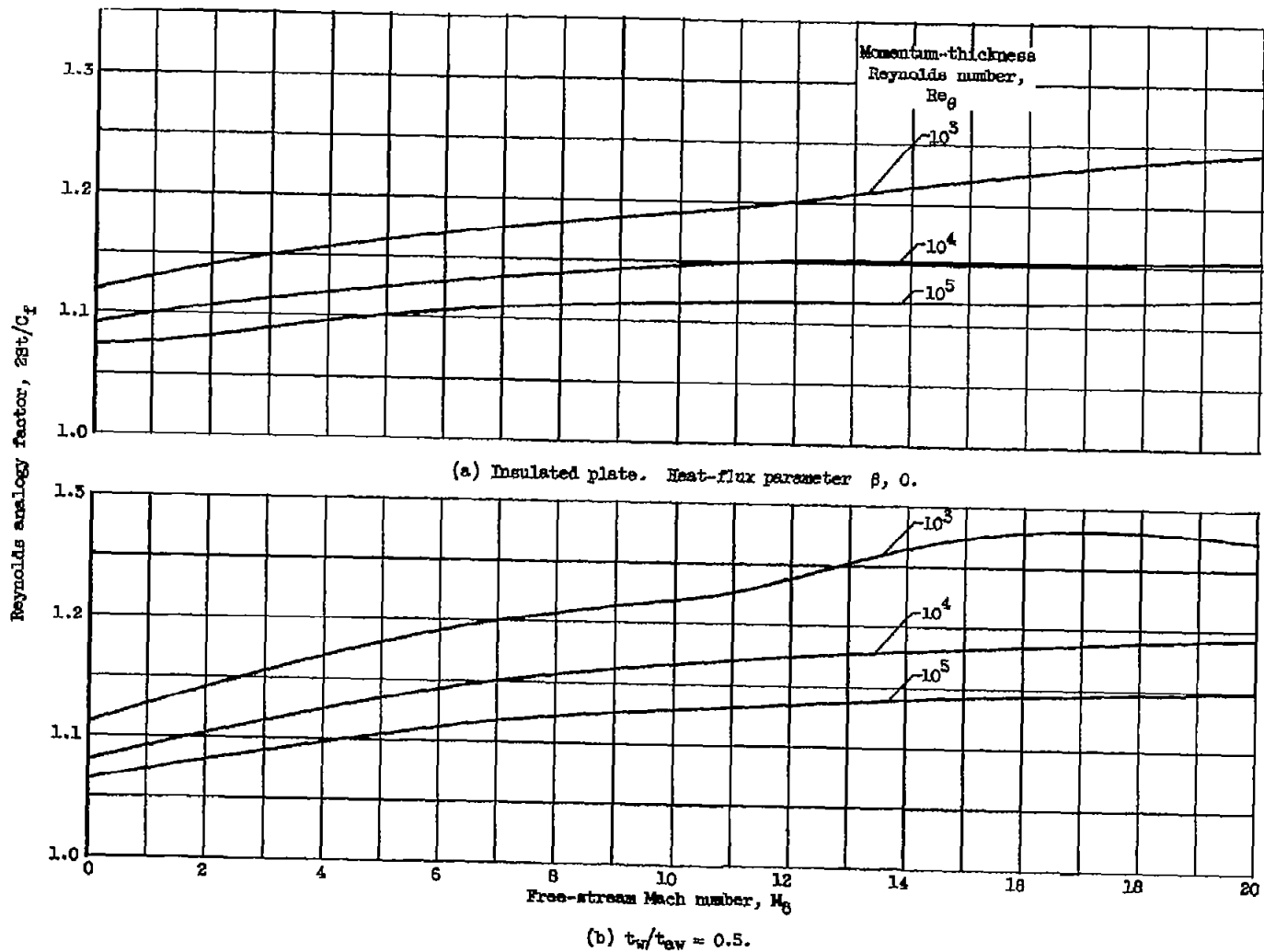
Figure 17. - Predicted variation of Reynolds analogy factor with momentum-thickness Reynolds number and Mach number. Prandtl number, 0.75.

4616
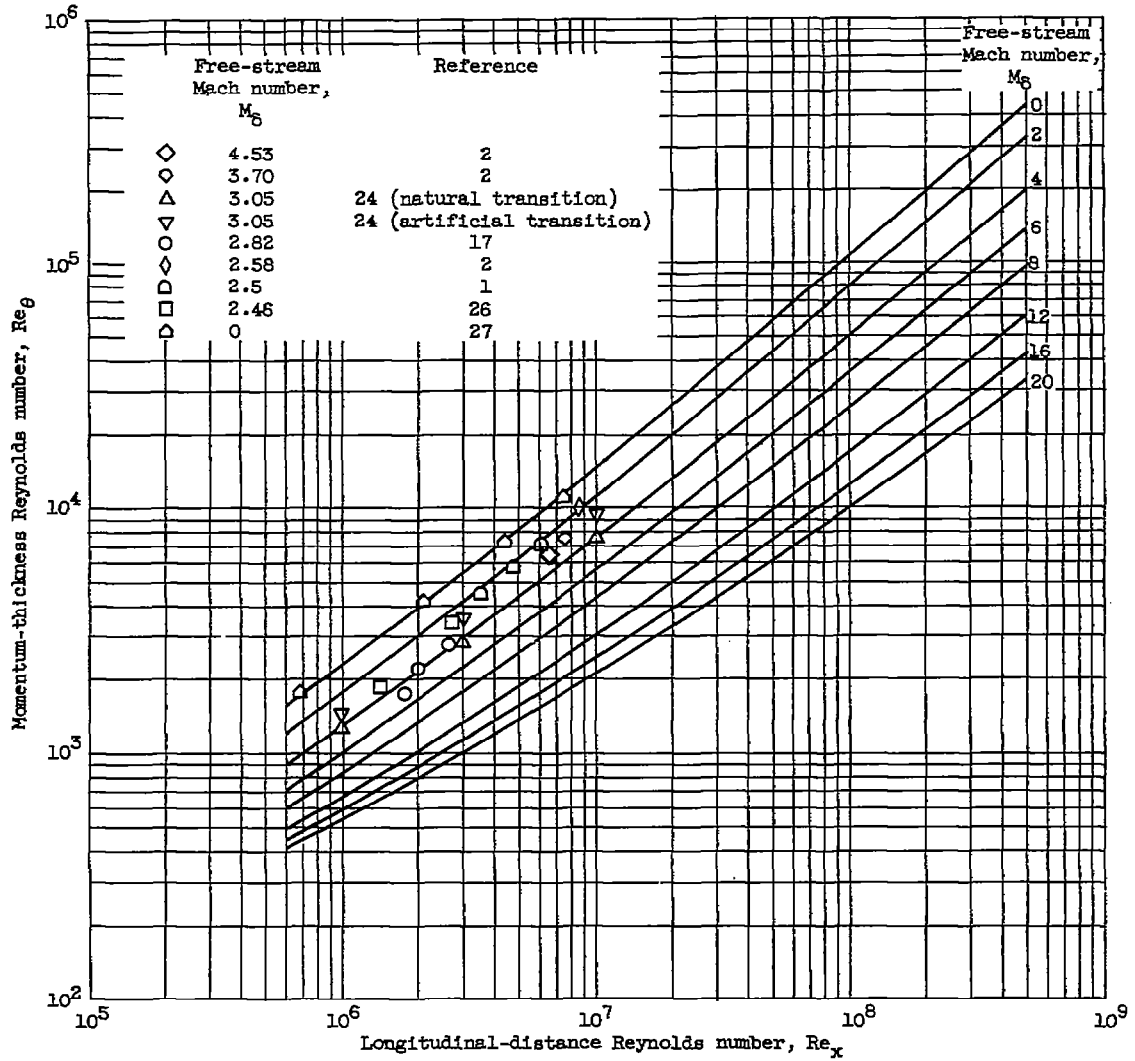
Figure 18. - Predicted variation of momentum-thickness Reynolds number with longitudinal-distance Reynolds number and Mach number for insulated plate and comparison with experiment. Prandtl number, 0.73; heat-flux parameter β, 0.
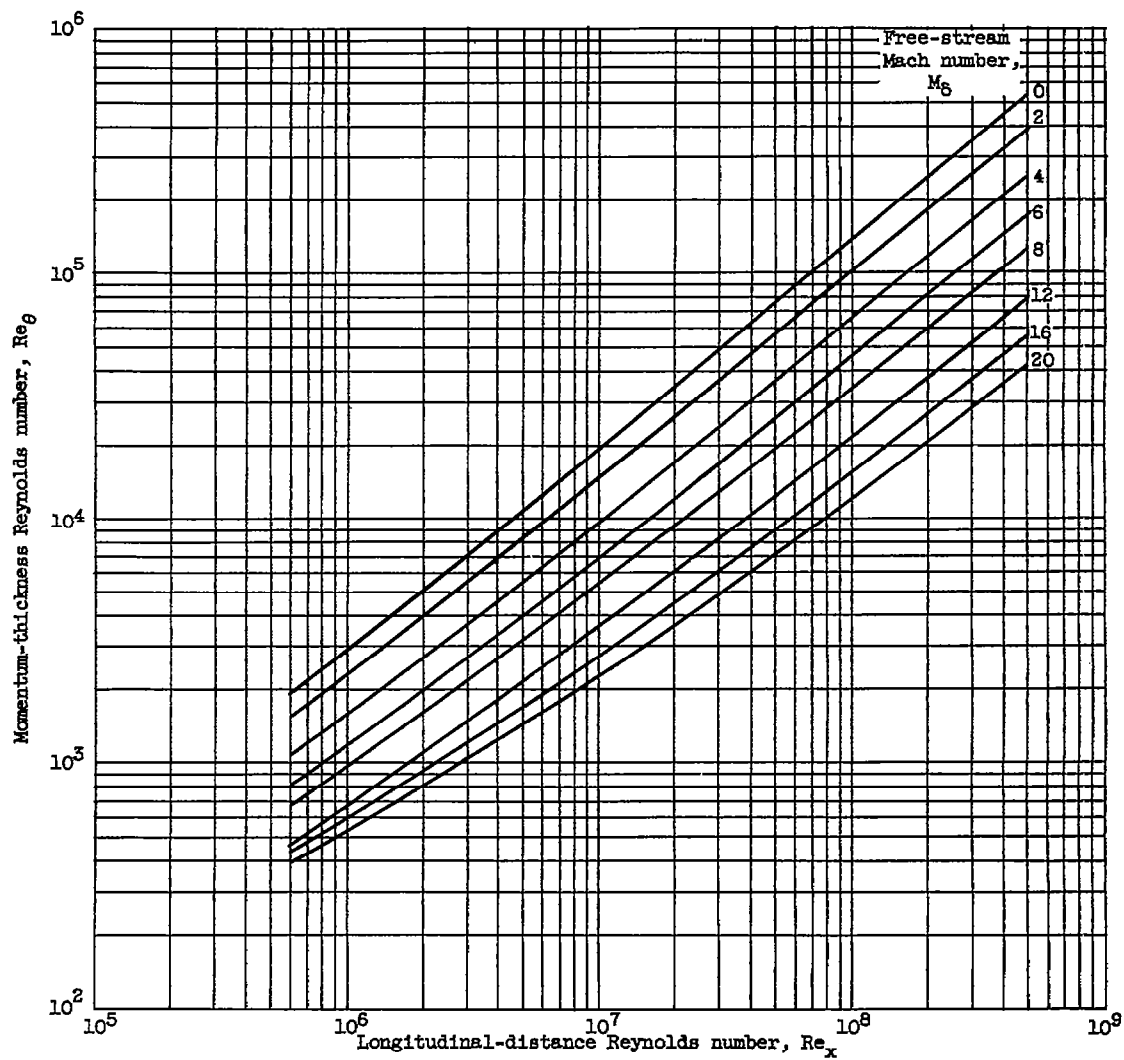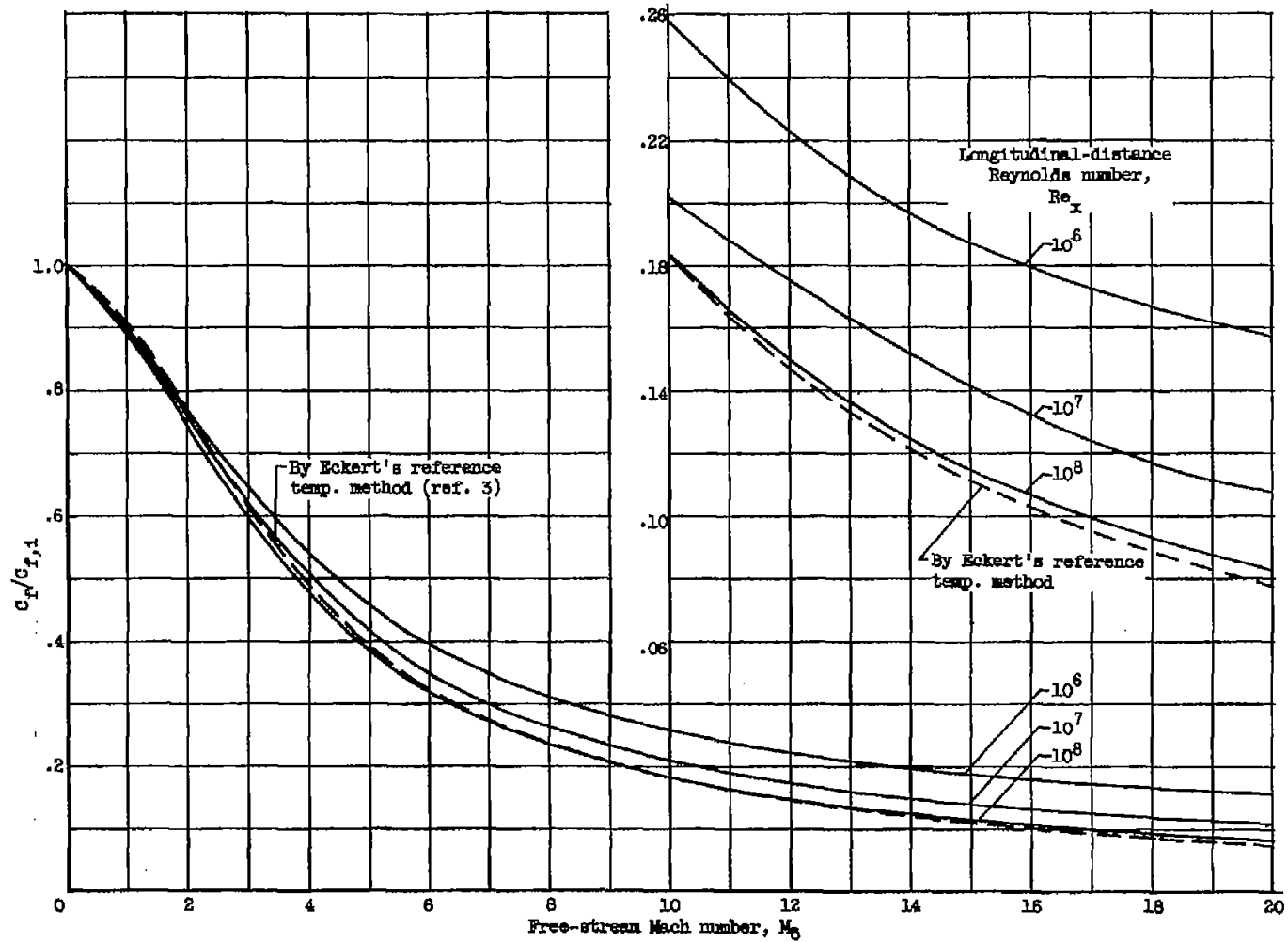
Figure 19. - Predicted variation of momentum-thickness Reynolds number with longitudinal-distance Reynolds number and Mach number for t_w/t_{aw} of 0.5. Prandtl number, 0.73.
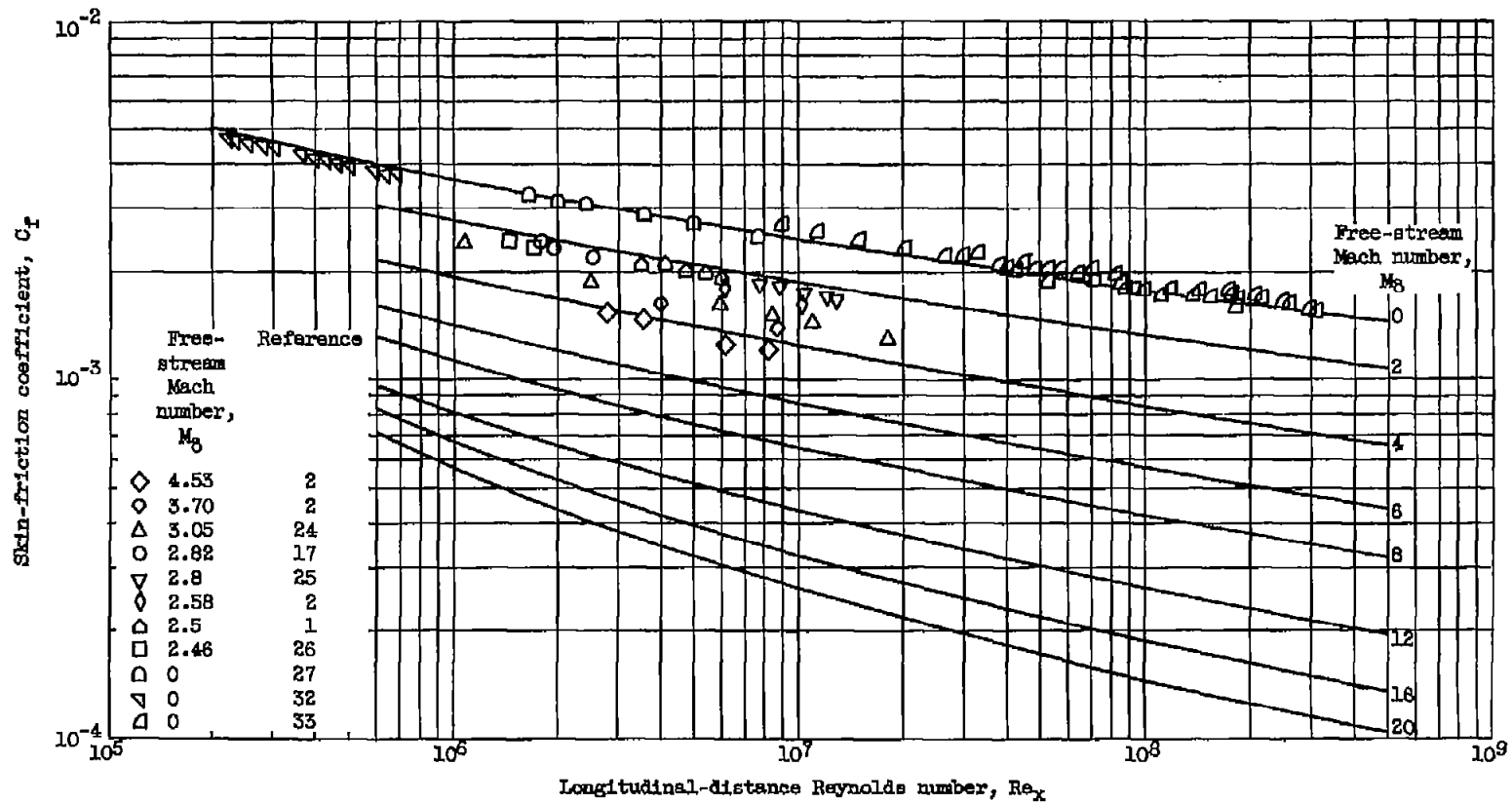
Figure 20. - Predicted variation of skin-friction coefficient with longitudinal-distance Reynolds number and Mach number for insulated plate and comparison with experiment. Prandtl number, 0.73; heat-flux parameter β, 0.

Figure 21. – Variation of $C_f/C_{f,i}$ with Mach number for various values of longitudinal-distance Reynolds number for insulated plate. Prandtl number, 0.73; heat-flux parameter β, 0.
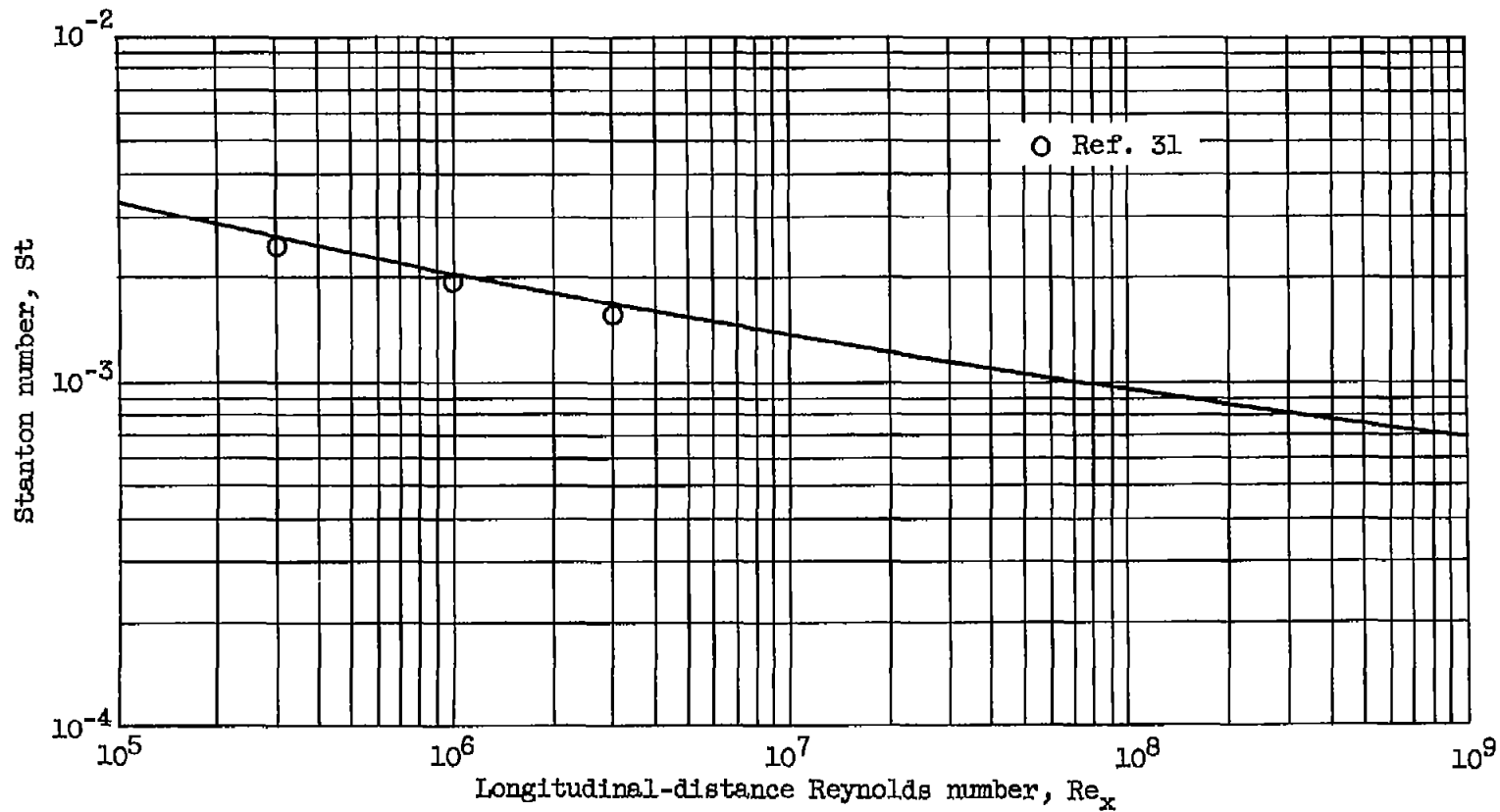
Figure 22. - Predicted variation of Stanton number with longitudinal-distance Reynolds number for insulated plate and comparison with experiment for low-speed flow. Prandtl number, 0.73; Mach number, 0.
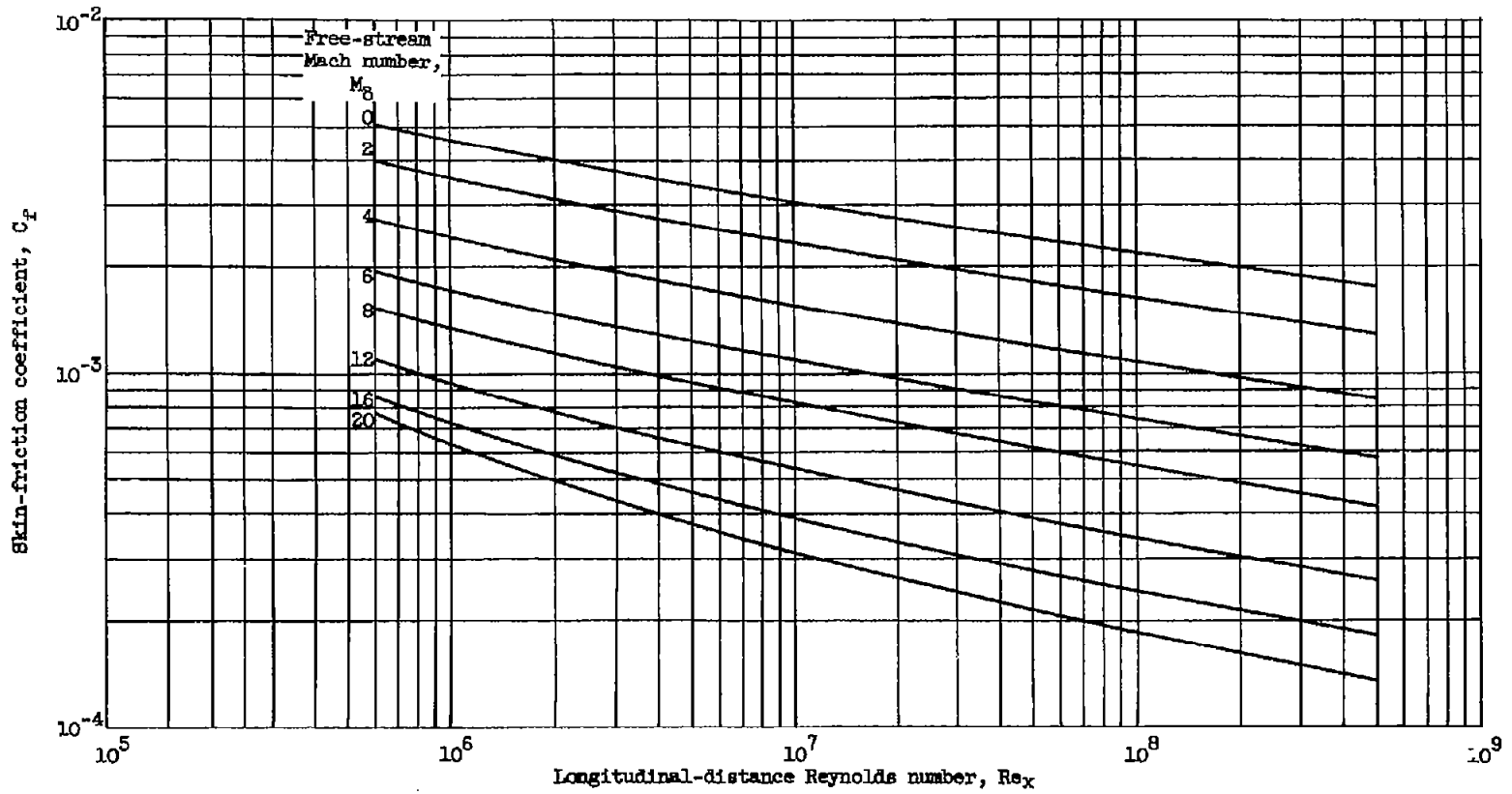
Figure 23. - Predicted variation of skin-friction coefficient with longitudinal-distance Reynolds number and Mach number for t_w/t_{aw} of 0.5. Prandtl number, 0.73.
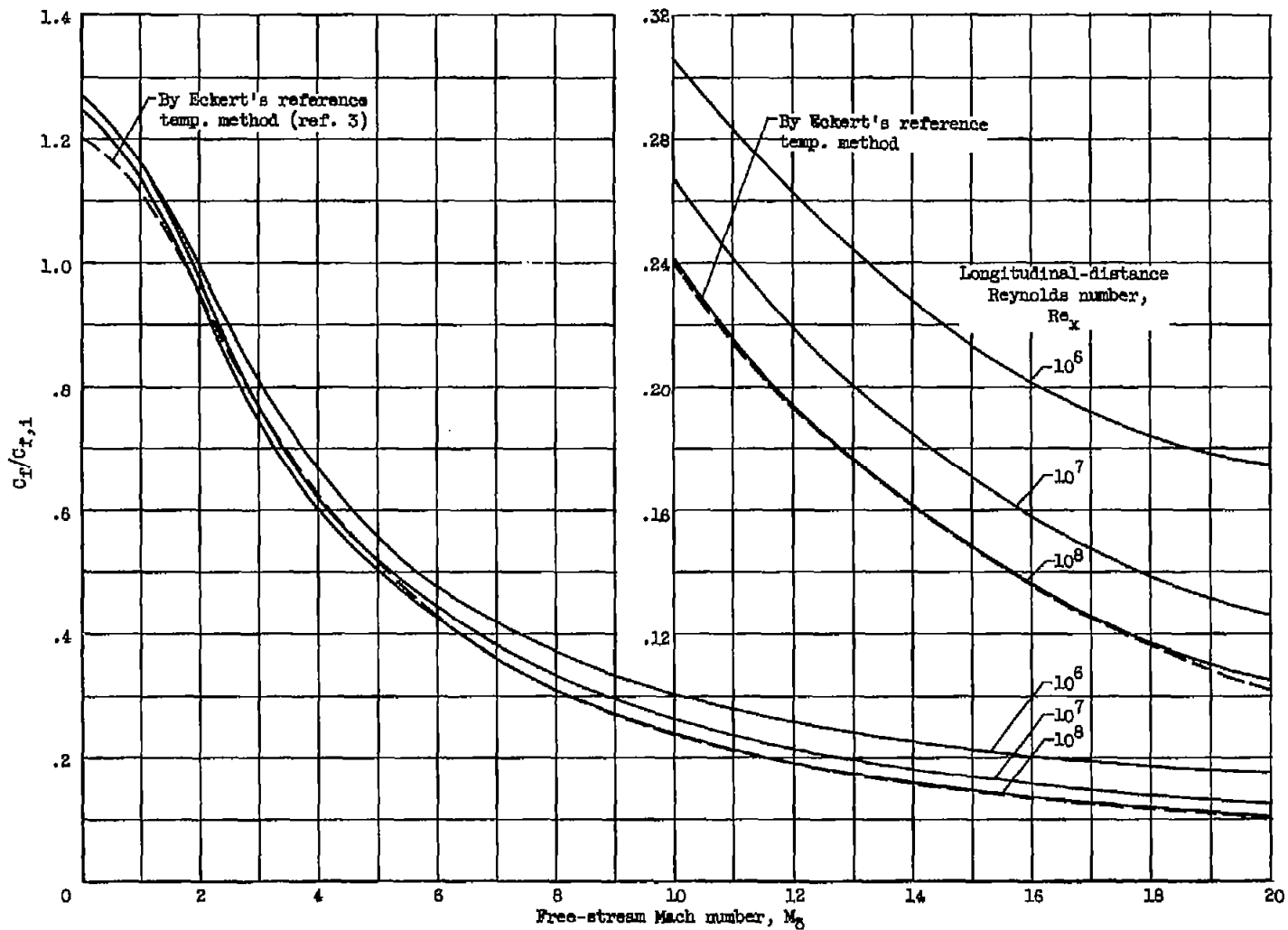
Figure 24. - Variation of $C_f/C_{f,1}$ with Mach number for various values of longitudinal-distance Reynolds number and t_w/t_{aw} of 0.5. Prandtl number, 0.73.